Constraining Cosmological Parameters

Ashutosh Tripathi

A dissertation submitted for the partial fulfilment of BS-MS dual degree in Science

Indian Institute of Science Education and Research Mohali

April 2014

Certificate of Examination

This is to certify that the dissertation titled "**Constraining Cosmological Parameters**" submitted by Mr. Ashutosh Tripathi (Reg. No. MS09031) for the partial fulfilment of BS-MS dual degree programme of the Institute, has been examined by the thesis committee duly appointed by the Institute. The committee finds the work done by the candidate satisfactory and recommends that the report be accepted.

Prof. J.S.Bagla Dr. Sanjeev Kumar Dr. H.K. Jassal

(Supervisor)

Dated : 25 April 2014

Declaration

The work presented in this dissertation has been carried out by me under the guidance of Dr. H. K. Jassal at the Indian Institute of Science Education and Research Mohali.
This work has not been submitted in part or in full for a degree, a diploma, or a fellowship to any other university or institute. Whenever contributions of others are involved, every effort is made to indicate this clearly, with due acknowledgement of collaborative research and discussions. This thesis is a bonafide record of original work done by me and all sources listed within have been detailed in the bibliography.

(Ashutosh Tripathi)

(Candidate)

In my capacity as the supervisor of the candidate's project work, I certify that the above statements by the candidate are true to the best of my knowledge.

(Dr. H. K. Jassal)

(supervisor)

Acknowledgement

Finishing a M.S. in physics is truly a marathon event, and it would have not been possible for me to finish this long and interesting journey without the help of countless people that were around me in last five years. Some of them were not with me physically during this period, but they are in my heart all the time. I must first express my gratitude towards my advisor Harvinder Kaur Jassal. She is an outstanding mentor and teacher. Her leadership, support, guidance, attention to detail, hard work, patience and kindness have set an example I hope to match some day. Thank you for your help and guidance. I would like to thank Jasjeet Singh Bagla from whom I have learned a lot. He taught me more than I could read in any book on physics. He is always in his office and very welcoming. I would like to thank Sanjeev Kumar for valuable advise regarding research. I would like to thank my colleague Archana Sangwan, who helped me a lot in understanding cosmology and in correcting the algorithms. Thanks Archanaji.
I also want to say thanks to my fellow postdoctoral students Shruti Thakur, Nisha Gupta and Neetika Gaur for having very helpful discussions with me during my research. I am extremely fortunate to have an enthusiastic and talented proofreaders in the form of Suma N Murthy and Archana Sangwan. Their sharp eyes and hard work did much to make this thesis better. Any remaining errors or omissions are obviously the sole responsibility of mine. Special thanks to Anshul for helping me with the programming.
I would like to say thanks to my dear friends/seniors : Arnab Chakraborty and Ashwini Veigas who are not with me but they always encourage me and believe in me more than I do.
I want to give a very special thanks, though this word "thanks" is not enough for my best friends Ashish Meena, Gaurav Verma and Ashutosh Tiwari for making my life in the institute funny and interesting.

Finally, and most importantly, this work would not have been possible without the endless support and encouragement from my parents. My younger brother Saurabh taught me some very important things of life which I eventually missed. I dedicate this thesis to my elder sister **Nisha Tripathi** who has been a great inspiration since forever. She saved me from all adversities of life in the past and inspire me to face them in the future.
I will always remember the wonderful time that I spend here with my friends, students and teachers of IISER-Mohali. Above all, I thank God for everything.

Contents

List of Figures

Chapter 1

Introduction

The universe is expanding and its expansion rate changes with time. The rate is initially decelerating because of the dominance of matter density and later it starts accelerating. A number of observations now support the idea that the universe is spatially flat and there is accelerated expansion. Many cosmologists believe that the dark energy is responsible for this accelerated expansion. The cosmological constant models is the simplest model but it has severe fine tuning problem. To overcome these difficulties, other dark energy models have been proposed. Two of these models, XCDM parametrisation with constant w and w as a function of redshift and non-flat universe model have been used. observational data are used to constrain their parameter sets. Finally, the basic definition of dark energy term is used to consider the model of accelerating universe driven by scalar fields whose dynamics is determined by the potential. Then, the new form of dark energy density is obtained and will be fitted with observations for various cosmological models.

In this thesis, we describe background cosmology, Friedmann's equations, distance measures in cosmology and their observational consequences. In the following chapter, we explain data analysis techniques used in the analysis. In chapter 3, we discuss why we used these particular data sets: measurements of the Hubble parameter H(z), Supernova (SN) apparent magnitudes, and the baryonic acoustic oscillations (BAO) peak length scale, as functions of redshift z; for constraining the cosmological parameters. In chapter 4, we constrain the different models of cosmology using various observations. We used the particle physics Quintessence scalar field model to determine w

theoretically and then constrain its value with the observations.

1.1 Dynamics of the Friedmann Model

A universe which is spatially homogeneous and isotropic at each instant of time is described by the Friedmann-Robertson-Walker metric given by

$$ds^2 = dt^2 - a^2(t)\left(\frac{1}{1-kr^2}dr^2 + r^2(d\theta^2 + sin^2\theta d\phi^2)\right) \tag{1.1}$$

The Friedmann metric contains the constants k and a which are determined by the Einstein's equations

$$G_i^k = R_i^k - \frac{\delta_i^k R}{2} = 8\pi G T_i^k \tag{1.2}$$

The assumption of isotropy requires T_0^μ must be zero and the spatial components T_i^k must have a diagonal form with all have equal value. Homogeneity requires all the components to be independent of the spatial coordinate. Such a stress tensor can be written as

$$T_i^k = dia[\rho(t), -p(t), -p(t), -p(t)] \tag{1.3}$$

ρ is the enrgy density and p is pressure density. Solving Einstein's equation with the above definition of stress tensor give two independent equations

$$\frac{\dot{a}^2 + k}{a^2} = \frac{8\pi G\rho}{3} \tag{1.4}$$

$$\frac{2\ddot{a}}{a} + \frac{\dot{a}^2 + k}{a^2} = -8\pi G p \tag{1.5}$$

these equation along with the equation of state $p = p(\rho)$ determine three unknowns in the above equations. The value of k from the above equations is

$$\frac{k}{a^2} = \frac{8\pi G\rho}{3} - \frac{\dot{a}^2}{a^2} = \frac{\dot{a}^2}{a^2}[\frac{\rho}{(3H^2/8\pi G)} - 1] \tag{1.6}$$

The various variables in the equation is defined as

$$H(t) = \frac{\dot{a}}{a}, \qquad \rho_c = 3H^2(t)/8\pi G, \qquad \Omega(t) = \frac{\rho}{\rho_c} \tag{1.7}$$

Using the above definition to rewrite the equation and evaluating at $t = t_0$, we get

$$\frac{k}{a_0^2} = H_0^2(\Omega - 1) \tag{1.8}$$

The subscript 0 defines the value of parameters at $t = t_0$ i.e. at present time. Substituting the value of $(\dot{a}^2 + k)/a^2$ from equation (1.12) into (1.13), we get

$$\frac{\ddot{a}}{a} = \frac{4\pi G}{3}(\rho + 3p) \tag{1.9}$$

For normal matter, $\rho + 3p > 0$, $\ddot{a} < 0$. In other words a will be smaller in the past and will become zero at sometime. The time coordinate is chosen in such a way that time t at which a becomes zero is taken to be 0 i.e. a and t are zero. In that case, the present age of the universe satisfy the inequality $t_0 < t_{univ}$ where

$$t_0 = H_0^{-1} = 9.8 \times 10^9 h^{-1} s \tag{1.10}$$

The value of h varies from 0.5 to 1.0.

1.2 Solving the Einstein's Equation

We can write eq. (2.12) as $\rho a^3 = (3/8\pi G)a(\dot{a}^2 + k)$. Differentiating this equation and using eq.(2.13), we get

$$\frac{d(\rho a^3)}{dt} = -3a^2 p \tag{1.11}$$

If we take the equation of state to be $p = w\rho$,we get

$$\rho \propto a^{-3(1+w)} \tag{1.12}$$

In particular, $w = 0$ for non relativistic matter and $w = 1/3$ for radiation. Therefore, the corresponding densities varies as

$$\rho_{NR} \propto a^{-3} \qquad and \qquad \rho_R \propto a^{-4} \tag{1.13}$$

By Solving eq.(1.19) for $\dot{a}$ and a , we get

$$\dot{a} \propto a^{\frac{-1(1+3w)}{2}} \qquad and \qquad a \propto t^{\frac{2}{3(1+w)}} \tag{1.14}$$

for non relativistic case, $a \propto t^{2/3}$ and for radiation $a \propto t^{1/2}$

The total energy density of the universe can be expressed as

$$\rho_{total} = \rho_r(a) + \rho_n(a) + \rho_v(a) = \rho_c \left(\Omega_r(\tfrac{a_0}{a})^4 + \Omega_n(\tfrac{a_0}{a})^3 + \Omega_v\right) \tag{1.15}$$

substituting this into Einstein's equation, we get

$$\frac{\dot{a}^2 + k}{a^2} = H_0^2 \left(\Omega_r \left(\frac{a_0}{a}\right)^4 + \Omega_n \left(\frac{a_0}{a}\right)^3 + \Omega_v\right) \tag{1.16}$$

We can write the value of k from eq.(1.16) and move it to right hand side. Introducing a dimensionless time coordinate $\tau = H_0 t$ and writing $a = a_0 q(\tau)$, the equation becomes

$$\left(\tfrac{dq}{d\tau}\right)^2 + V(q) = E \tag{1.17}$$

Where

$$V(q) = -\left(\tfrac{\Omega_r}{q^2} + \tfrac{\Omega_n}{q} + \Omega_v\right) \qquad and \qquad E = (1 - \Omega) \tag{1.18}$$

For the models $\Omega = \Omega_n + \Omega_v = 1$, we can take E = 0 and the equation to be solved is $dq/d\tau = \sqrt{V(q)}$. At high redshift, the universe is dominated by radiation and $\dot{q}$ is independent of the other cosmological parameters. At low redshift,the presence of cosmological constant constant makes a difference and velocity changes from decreasing to increasing function.
In the early evolution of the universe,the radiation term will dominate the dynamics and the solution is given by

$$q = \sqrt{2H_0 t}\sqrt[4]{\Omega_r} \tag{1.19}$$

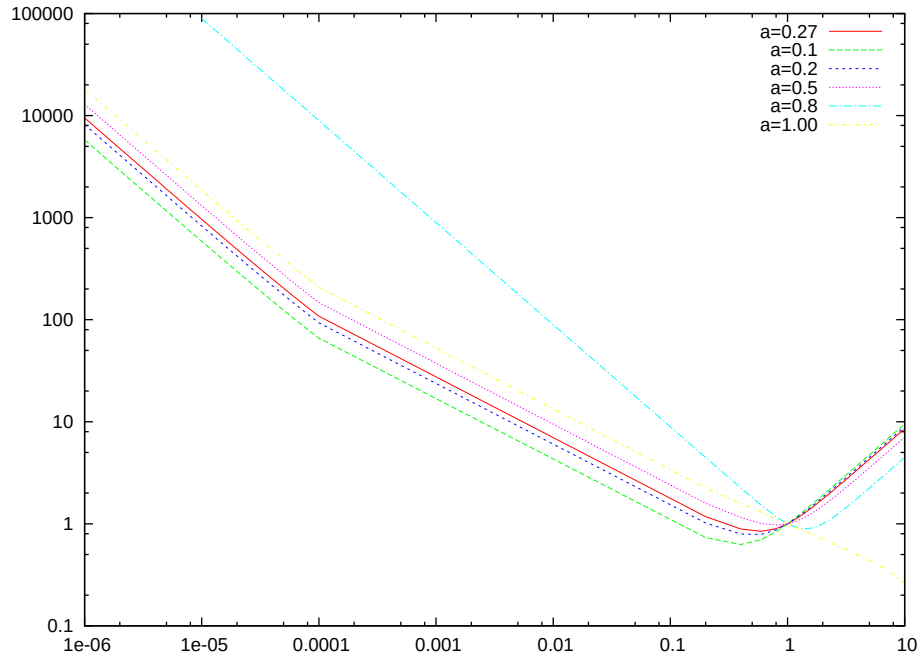

Figure 1.1: The "velocity" of the universe plotted against the "position" for different cosmological models. Here, a represents Ω_{nr}

Therefore for small a, we have $a \propto t^{1/2}$.
As the universe evolves, the matter density will catch up with the radiation density and the first two terms of the eq.(1.23) become important. When both radiation and matter densities are taken into consideration and other terms are ignored, eq.(1.26) has the solution

$$Ht = \frac{2\sqrt{2}}{3}\left((q-2)\sqrt{q+1}+2\right) \tag{1.20}$$

If $\Omega_v > \Omega_n$,then the vacuum density will dominate over other densities.Keeping only the Ω_v and Ω_n terms in eq.(1.18) and solving it, we get

$$q = 3\left(\frac{\Omega_n}{\Omega_v}\right)^{1/3} sinh^{2/3}\left(\frac{3\sqrt{\Omega_v}H_0 t}{2}\right) \tag{1.21}$$

when $\sqrt{\Omega}H_0 t << 1$, this reduces to the matter dominated evolution with $a \propto t^{2/3}$ and when it is much greater than 1, the growth is exponential with

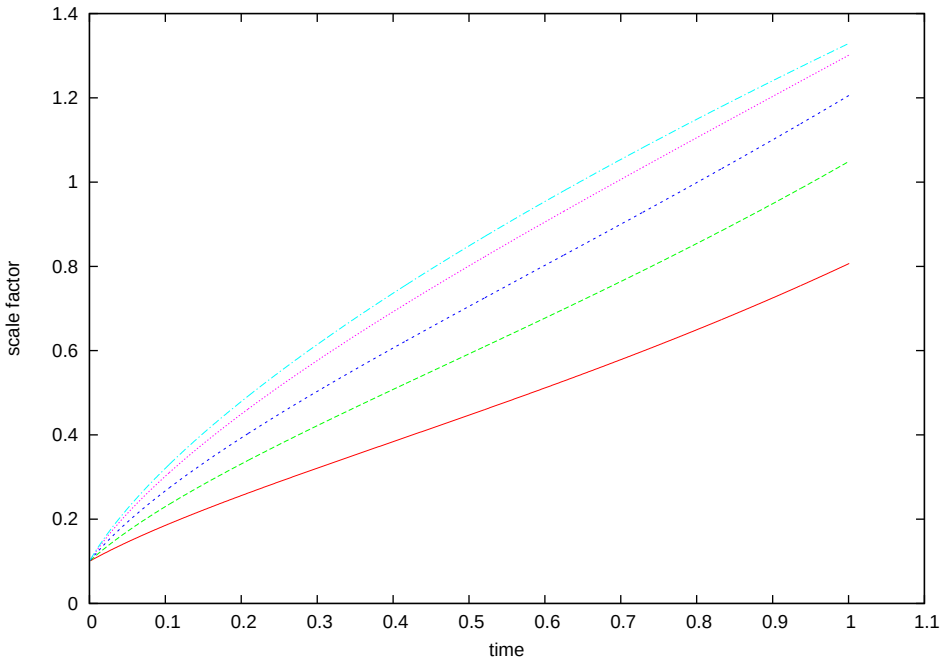

Figure 1.2: The scale factor of the universe plotted against the time for different cosmological models with all three parameters

$a \propto exp^(\sqrt{\Omega}H_0 t)$. In this case, the age at any given redshift t(z) is given by

$$t(z) = H_0^{-1} \frac{2}{3\sqrt{\Omega_v}} sinh^{-1}\left(\sqrt{\frac{\Omega_v}{\Omega_n}}(1+z)^{-3/2}\right) \tag{1.22}$$

At low redshift, we can ignore the radiation completely. The evolution now depends on the value of Ω_v and k. Let us take the case $\Omega_v = 0$ first. solving the eq.(1.23), we get

$$t(z) = H_0^{-1} \frac{\Omega}{2(1-\Omega)^{3/2}} \left(\frac{2(1-\Omega)^{1/2}(\Omega z+1)^{1/2}}{\Omega(1+z)} - cosh^{-1}(\frac{\Omega z-\Omega+2}{\Omega z+\Omega})\right) \tag{1.23}$$

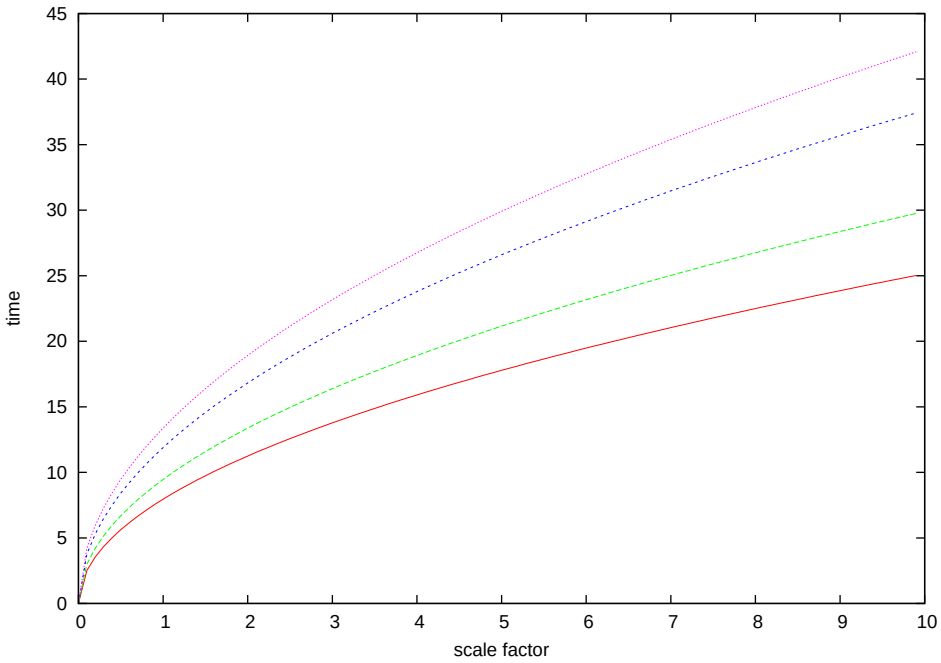

Figure 1.3: Plot of q as a function of time in the radiation dominated universe

1.3 Hubble Distances and Redshift of Galaxies

Hubble showed that the galaxies are moving away from us and measured distance r and showed that

$$v \propto r \tag{1.24}$$

It means farther the galaxy, the faster it is receding from us. This phenomenon was observed as a redshift of a galaxy's spectrum. This redshift appeared to have a larger value for fainter, presumably farther away, galaxies.Redshifted means going away and blueshifted means coming close. Consider two galaxies separated by the distance r, then the relative velocity $v \propto r$, this is called Hubble's law and mathematically given as

$$\vec{v} = H_0 \vec{r} \tag{1.25}$$

Where H_0 is the Hubble constant which relates the distance of the galaxy to its recession velocity. It can also be used to determine the size of observable

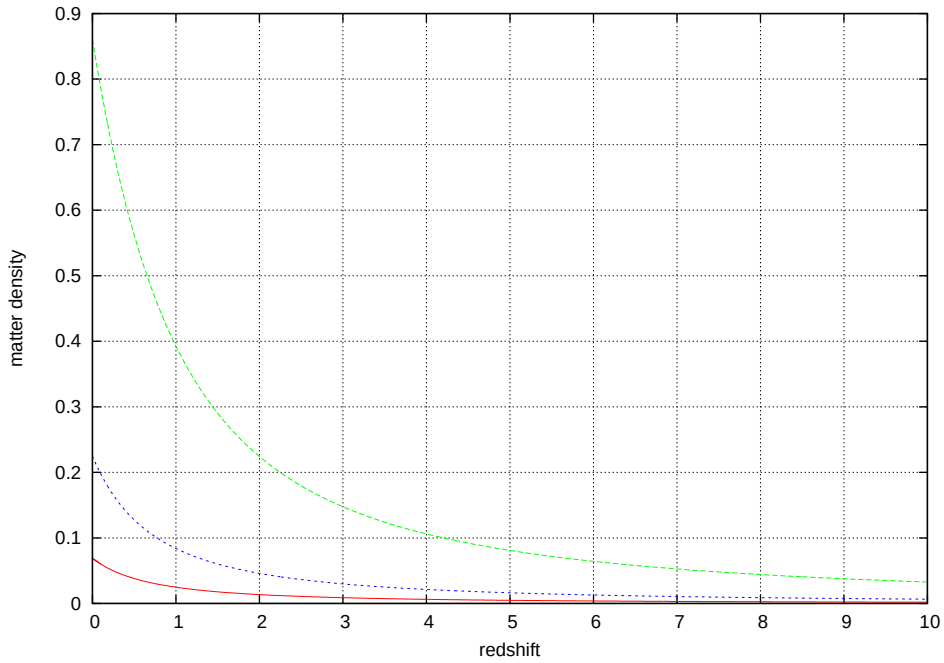

Figure 1.4: The age of the universe at a redshift z for model $\Omega_n + \Omega_v = 1$ with $\Omega_n = (0.2, 0.35, 0.5)$ from top to bottom.

universe and its age. It indicates the rate at which universe is expanding. The general form of this law is

$$v(t) = H(t)r(t) \tag{1.26}$$

H(t) is the value of Hubble constant whose current value is H_0. The current value of Hubble constant is H $\pm\sigma_H$= 68 $\pm$ 2.8 kms^{-1}Mpc^{-1}.
Cosmological principle states that no position in the space is special. We can infer from above that the hubble law is the violation of Cosmological Principle because according to it,all galaxies are receding from us and this will placed us at the special location in the universe. But it is also true for the observer observing from any other location in the universe. In this way, Cosmological principle is preserved.
We define some important quantities below:

1. **Physical or Proper Distance** : The actual distance between the two points in space is physical distance. It is donated by $\vec{r}(t)$

2. **Comoving or Co-ordinate distance**: This is just the label of the point in space and it is independent of time. It is denoted by $\vec{x}$.

   Physical and coordinate distance are related through

   $$\vec{r}(t) = a(t)\vec{x} \tag{1.27}$$

   Where a(t) is time dependent scalar which describes the expansion(or contraction) of the universe.

3. **Scale factor** a(t) is a dimensionless function of time that carries important information about the cosmological expansion of Universe. The current value of the scale factor is denoted by $a(t_0) = a_0$ and its value is often set to 1. The evolution of the scale factor is governed by general relativity. Differentiating the above equation with respect to time, we get

   $$v(t) = \dot{a}(t)\vec{x} \tag{1.28}$$

   $$\implies \frac{\dot{a}(t)}{a(t)}a(t)\vec{x} = \frac{\dot{a}(t)}{a(t)}\vec{r}(t) \tag{1.29}$$

   Using eq.(1.15), we can write H(t) as

   $$H(t) = \frac{\dot{a}(t)}{a(t)} \tag{1.30}$$

   Where over-dot represent time-derivative.Current evidences suggest that universe is accelerating which means $\dot{a}$(t) is increasing over time ($\ddot{a}$ is positive).

4. **Redshift** : When the galaxies move relative to us, we observe change in the wavelength of the light emitted by those galaxies. To describe this, it is convenient to define a redshift denoted by z. The redshift is a dimensionless quantity defined as the change in the wavelength of the light divided by the rest wavelength of the light:

   $$z = \frac{\lambda_0 - \lambda_e}{\lambda_e} \tag{1.31}$$

Where λ_e is the wavelength of the emitted wave and λ_0 is the wavelength of the observed wave. Redshift is a quantity which is related to a(t) as

$$1 + z = \frac{a(t_0)}{a(t)} = \frac{1}{a(t)} \tag{1.32}$$

Where we take the convention $a(t_0) = a_0 = 1$.
The redshift we observe for a distant object depends only on the relative scale factors at the time of emission and the time of observation. It does not depend on how the transition between a(t_e) and a(t_0) was made.

1.4 Friedmann model

The form of relations (1.30) and (1.31) at $z = 0$ and $a = a_0$ gives the age of universe. There are two Friedmann models that are of special interest in cosmology.

1. $\Omega_v = 0$ model which makes transitions from radiation-dominated to matter-dominated evolution. At the latter matter-dominated phase, it is characterized by a single parameter Ω_n. At $z = 0$ and $a = a_0$, eq.(1.31) becomes

$$H_0 t_0 = \frac{\Omega}{2(1-\Omega)^{3/2}}\{\frac{2(1-\Omega)^{1/2}}{\Omega} - cosh^{-1}\{\frac{2-\Omega}{\Omega}\} \tag{1.33}$$

2. $k = 0$ model, where both matter and vacuum density is non-zero. As radiation density is negligible, this model essentially has $\Omega_v + \Omega_n = 1$. At $z = 0$ and $a = a_0$, eq.(1.32) becomes

$$H_0 t_0 = \frac{2\Omega_v^{-1/2}}{3} ln \frac{1 + \sqrt{\Omega_v}}{\sqrt{\Omega_n}} \tag{1.34}$$

when both Ω_v and Ω_n are present and are arbitrary, the age of the universe is determined by the integral

$$H_0 t_0 = \int_0^\infty \frac{dz}{(1+z)\sqrt{(1+z)^2(1+\Omega_n z) - z(2+z)\Omega_v}} \tag{1.35}$$

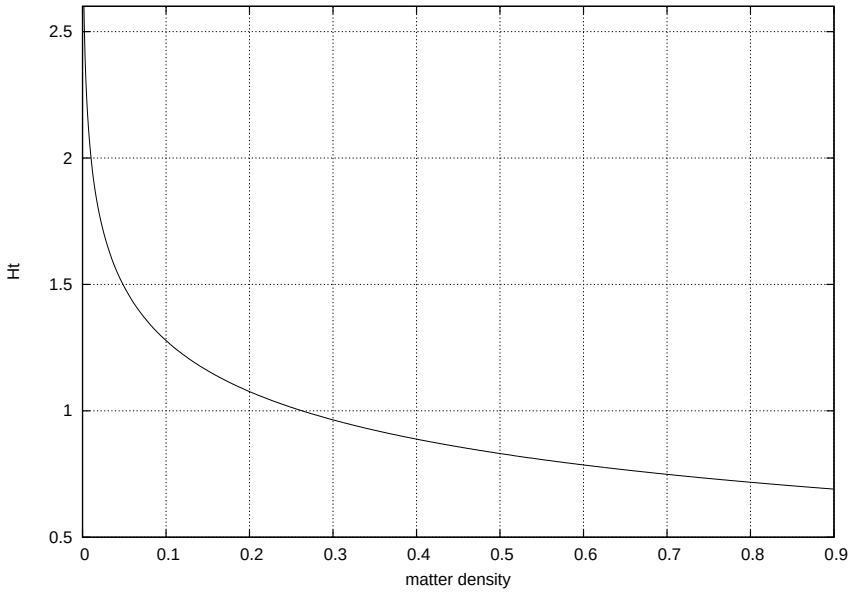

Figure 1.5: Curves of age in the Ω_n-H_0t_0 plane for (2) model.The x-axis is H_0t_0 and y-axis is Ω_n

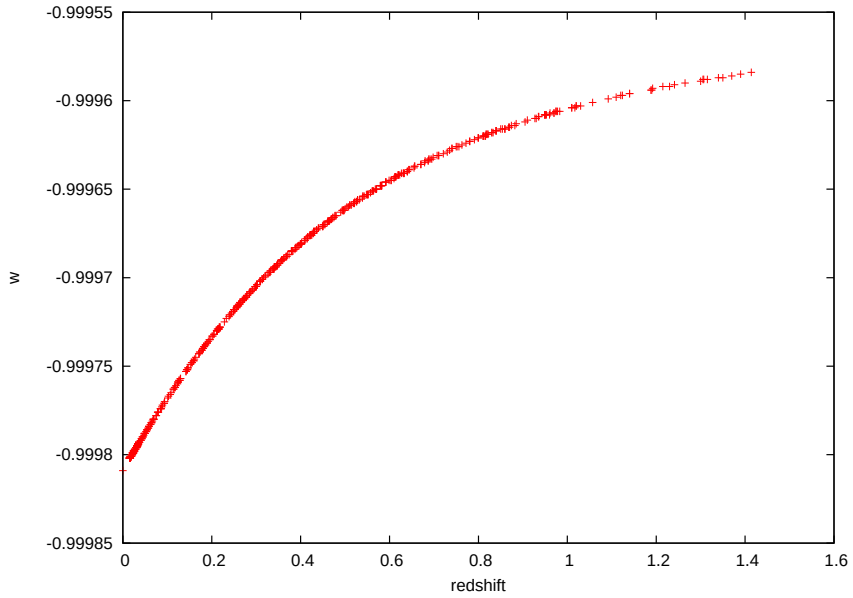

Figure 1.6: The age of the universe when both matter and vacuum density are arbitrary. The above plot shows it for $\Omega_n = 0.35$ and $\Omega_v = 0.1$.

1.5 Cosmological length scales

Let an observer located at $r = 0$ receive at time $t = t_0$ radiation from a source located at r_s. This radiation must have been emitted at some earlier time t_e such that the events (t_e, r_s) and $(t_0, 0)$ are connected by null geodesics. Taking the propagation of the ray to be along $\theta = constant$ and $\phi = constant$, the equation for null geodesics can be written as

$$0 = ds^2 = dt^2 - a(t)^2 \frac{dr^2}{1 - kr^2} \tag{1.36}$$

Integration of the above equation will give the relation between r_s and t_e

$$\int_{t_0}^{t_e} \frac{dt}{a(t)} = \int_0^{r_s} \frac{dr}{\sqrt{1 - kr^2}} \tag{1.37}$$

the left-hand side is a definite function of time in a given cosmological model. As the redshift z is also a unique function of time, we can express the left hand side as function of z and hence r_s can be expressed as the function of z. The function r_s is of considerable use in observational astronomy, as it relates the radial distance of an object to the redshift at which the light is emitted. It is convenient to define a quantity called the hubble radius by

$$d_H(t) = d_H(z) = \left(\frac{\dot{a}}{a}\right)^{-1} \tag{1.38}$$

So,dt can also be written as

$$dt = \frac{dt}{da}\frac{da}{dz}dz = -d_H(z)\frac{dz}{1+z} \tag{1.39}$$

It is now possible to write Eq.(2.36) as

$$\frac{1}{a_0}\int_0^z d_H(z)dz = S_k^{-1}(r_s) \tag{1.40}$$

Where $S_k^{-1} = sinh^{-1}x$, x, $sin^{-1}x$ for $k = -1, 0, +1$ respectively.So, r_s can be written as

$$r_s(z) = S_k\alpha, \qquad \alpha = \frac{1}{a_0}\int_0^z d_H(z)dz \tag{1.41}$$

The quantity r_s plays an important role in

1. Relating the luminosity of distant objects with the observed flux.
2. The measurement of angular sizes of distant objects.

Let F be the flux received from a source of luminosity L when the photons from the source reach us with a redshift z. The flux can be expressed as

$$F = \frac{1}{(area)} \frac{dE_{rec}}{dt_{rec}} \tag{1.42}$$

using the fact that

1. $I/\omega^3$is invariant where I is the intensity and ω is the frequency of photon.
2. $I[\omega(1+z); z] = I(\omega, 0)(1+z)^3$
3. The proper area at $a = a_0$ of a sphere of comoving radius $r_s(z)$ is $4\pi^2 a_0^2 r_s^2$.

we get

$$F = \frac{1}{(4\pi^2 a_0^2 r_s^2)} \frac{1}{(1+z)^2} \frac{dE_s}{dt_s} = \frac{1}{(4\pi^2 a_0^2 r_s^2)} \frac{1}{(1+z)^2} L \tag{1.43}$$

That means $F = L/4\pi r^2$.It is now convenient to define the distance $d_L(z)$, called the luminosity distance by

$$d_L(z) = \sqrt{\frac{L}{4\pi F}} = a_0 r_s(z)(1+z) = a_0(1+z)S_k(\alpha) \tag{1.44}$$

Another observable parameterfor distant sources is the angular diameter. If D is the physical size of the object that subtends an angle δ to the observer, then for small δ, we have $D = r_s a(t_e)\delta$. The angular diameter distance $d_A(z)$ for the source is defined by the relation $\delta = D/d_A$, so $d_A(z)$ is

$$d_A(z) = r_s a(t_e) = a_0 r_s(t_e)(1+z)^{-1} \tag{1.45}$$

so we can see that

$$d_A(z) = d_L(z)(1+z)^{-2} \tag{1.46}$$

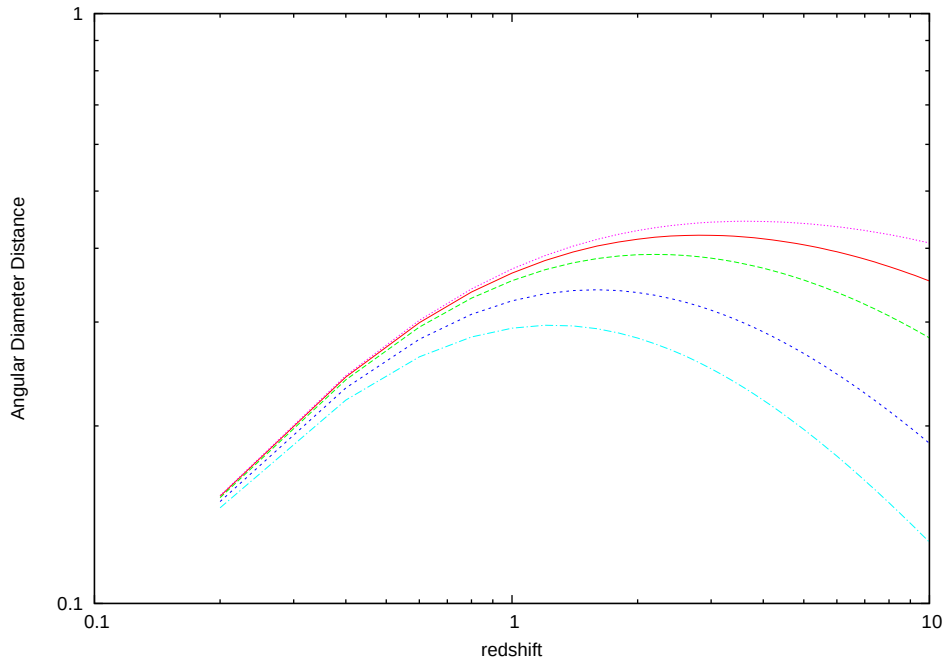

Figure 1.7: Angular diameter distance in units of cH_0^{-1} as a function of redshift for open model with different values of Ω_n

We can determine the quantity d_L by measuring the flux F for a class of objects for which the luminosity L is known. If we can also measure the redshift z for these objects, then a plot of d_L against z will allow us to determine the parameters H_0 and q_0.
We can write Eq.(1.26) as

$$d_H(z) = H_0^{-1}\left(\Omega_r(1+z)^4 + \Omega_n(1+z)^3 + \Omega_v + (1-\Omega)(1+z)^2\right)^{-1/2} \quad (1.47)$$

For the matter dominated universe with only Ω_n contributing to the energy density, the above equation can be written as

$$d_H(z) = H_0^{-1}(1+z)^{-1}(1+\Omega z)^{-1/2} \quad (1.48)$$

The r_s can be written as

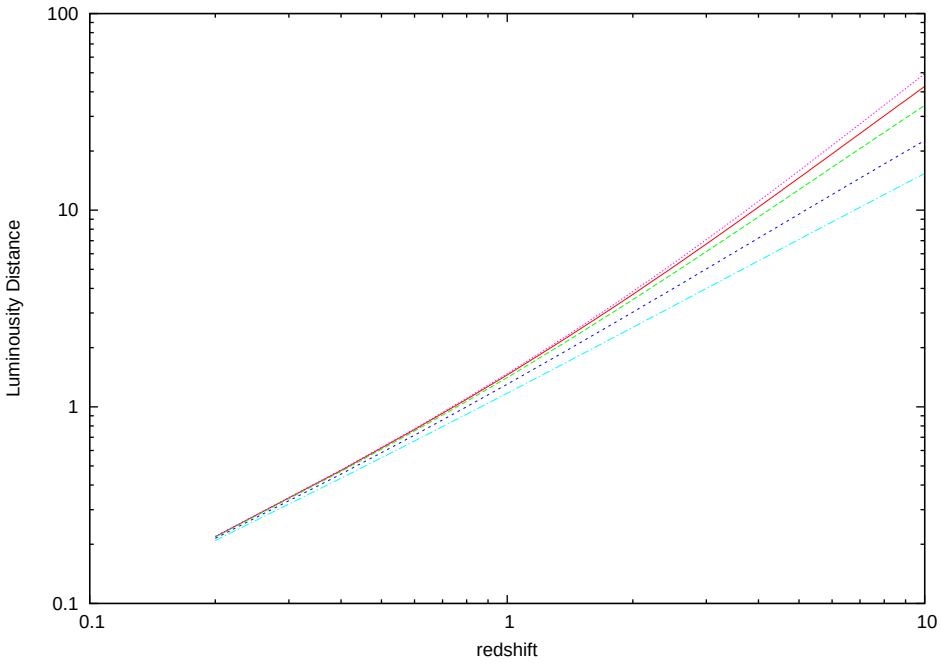

Figure 1.8: Luminosity diameter distance in units of cH_0^{-1} as a function of redshift for open model with different values of Ω_n

$$r_s(z) = \frac{2\Omega z + 2(\Omega - z)(\sqrt{\Omega z - 1} - 1)}{H_0 a_0 \Omega^2 (1+z)} \tag{1.49}$$

Using these, we can express the angular diameter distance in the form

$$d_A(z) = 2H_0^{-1}\Omega^{-2}[\Omega z + (\Omega - z)(\sqrt{1+\Omega z} - 1)](1+z)^{-2} \tag{1.50}$$

And the luminosity distance as

$$d_L(z) = 2H_0^{-1}\Omega^{-2}[\Omega z + (\Omega - z)(\sqrt{1+\Omega z} - 1)] \tag{1.51}$$

1.6 Distance Modulus

The apparent magnitude, m, of an astronomical object is defined by the ratio of the apparent flux of the object to some reference flux,

$$m = -2.5log_{10}\left(\frac{F}{F_{ref}}\right) \tag{1.52}$$

The absolute magnitude, M , is defined as the apparent magnitude the object would have if it were 10 pc away. The difference between them is known as distance modulus and can be expressed as:

$$\mu = m - M = -2.5log_{10}\left(\frac{F}{F_{ref}}\right) - (-2.5log_{10}\left(\frac{F_{10pc}}{F_{ref}}\right)) \tag{1.53}$$

Solving and using the definition of F($F = L/4\pi d_L^2$),L being the luminosity and using the fact that Luminosity of the celestial object is constant, we get

$$\mu = 5log_{10}\left(\frac{d_L}{10pc}\right) \tag{1.54}$$

This equation with appropriate scaling will be used in Supernovae analyses in Chapter 3.

Chapter 2

Data Analysis Techniques

In this chapter, we discuss the data analysis techniques used in the subsequent chapters.Mainly,we dicuss χ^2 minimization method,marginalization and confidence intervals.

Modeling of Data We choose or design a figure-of-merit function that measures the agreement between the data and the model with a particular choice of parameters. The parameters of the model are then adjusted to achieve a minimum in the merit function yielding best-field parameters. A fitting parameter should provide

1. Parameters

2. Error estimates on the parameter

3. A statistical measure of goodness-of-fit.

2.1 χ^2 Minimization

Suppose that we are fitting N data points (x_i, y_i) i=1,2,3.... to a model that has M adjustable parameters a_j j=1,2....m.The model predicts a functional relationship between the measured independent variables.

$$y(x) = y(x, a_1, a_2....a_m) \tag{2.1}$$

We want to minimize to get fitted value of a_j's.The method used to do so is least-square fit minimize over $a_1...a_m$.

$$\sum_{i=0}^{N}[y_i - y(x_i, a_1, ..., a_m)] \tag{2.2}$$

Maximum Likelihood Estimates We identify the probability of the data given the parameters as the likelihood of the parameters given the data.
Suppose each data point y_i has a measurement error that is independently random and has a distribution as a normal(Gaussian) distribution around the true model y(x) and suppose that the standard deviation σ of these normal distribution are same for all the points.Then the probability of data set is the product of possibilities of each point.

$$P \propto \prod_{i=1}^{N} exp[-\frac{1}{2}\left(\frac{(y_i - y(x_i))}{\sigma}\right)^2] \tag{2.3}$$

Maximizing this is equivalent to maximizing its logarithm or minimizing the negative of its logarithm.

$$\sum_{i=1}^{N}\frac{(y_i - y(x_i))^2}{2\sigma^2} - Nlog\Delta y \tag{2.4}$$

Central Limit Theorem: The probability distribution of the sum of a very large number of very small random deviation almost converges to normal distribution.
If each data points (x_i,y_i) has its own known standard deviation σ_i,then last equation is modified only by putting a subscript i on σ. The maximum likelihood estimate of model parameters is obtained by minimizing the quantity.

$$\chi^2 = \sum_{i=1}^{N}\left(\frac{y_i - y(x_i, a_1, .., a_m)}{\sigma}\right)^2 \tag{2.5}$$

χ^2 is a sum of N squares of normally distributed quantities, each normalized to unit variance. Once we have adjusted $a_1...a_m$ to minimize the value of χ^2, the terms in sum are not all statistically independent.
For instance, If we try to fit N data points to a straight line model $y = a+bx$,

then the expression used for χ^2 is

$$\chi^2 = \sum_{i=1}^{N} \left(\frac{y_i - a - bx_i}{\sigma_i} \right)^2 \tag{2.6}$$

If the measurement errors are normally distributed,then this function will give maximum likelihood.

2.2 Confidence Intervals

Confidence Intervals for an unknown parameter θ of some distribution are intervals $\theta_1 \leq \theta \leq \theta_2$ that contain θ_1 not with certainty but with a high probability.It essentially means that there is certain probability that the value exist within this range.Mainly 3 confidence intervals are used

1. 1σ interval which means there is 68% probability that the value lies within this range.
2. 2σ interval which means there is 95% probability that the value lies within the range.
3. 3σ interval which means there is 99% probability that the value lies within the range.

2.3 Marginalisation

Marginalisation is a technique in which we integrate the function over the whole range of a parameter in order to marginalised the dependence of function on that parameter. Mathematically

$$\int P(x, y, z)dz = P(x, y) \tag{2.7}$$

In the subsequent chapters, when the number of parameters will be more than 2, we will marginalised over the other **Nuisance Parameters** in order to get the plots for the desired ones.

Chapter 3

Dark Energy and Dark Energy Models

In this chapter, we discuss the observational evidences for dark energy and its dependence on redshift.Using supernovae data, we try to constrain the dark energy density using techniques discussed in the last chapter.

3.1 Observational Evidences

From the last few decades,the evidence for the presence of cosmological constant or dark energy has been steadily increasing which is believed to be the reason for the accelerating expansion of the universe. In order to explain it, we require the "substance" with value of state parameter $w < -1/3$.Newtonian gravity cannot account for the accelerated expansion, it allows only decelerated cosmological expansion.Let's consider a homogeneous sphere with radius a and energy density ρ. The Newton's equation of motion for a point particle with mass m on this sphere is

$$F = -\frac{GMm}{a^2}, m\ddot{a} = -\frac{Gm}{a^2}(\frac{4\pi a^3\rho}{3}) \Longrightarrow \frac{\ddot{a}}{a} = -\frac{4\pi G\rho}{3} \tag{3.1}$$

The difference compared to the Einstein's equation is the absence of the pressure term, P. This appears in Einstein's equation because of relativistic effects. The condition $w < -1/3$ means that we essentially require a large

negative pressure in order to give rise to an accelerated expansion.
Observational facts in the support of the existence of dark energy.

- The age of the Universe compared to that of the oldest star in combination with estimate of H_0.
- Supernovae apparent magnitude observations (SNeIa)
- Cosmic microwave background (CMB) anisotropy observations in combination with the estimation of Ω_{m0} , the non relativistic matter density parameter.
- Baryonic acoustic oscillation (BAO) peak length scale measurements.
- Hubble parameter measurements.
- Large-scale-structure (LSS) observations.

Out of the above,we will discuss the supernovae, BAO and Hubble parameters observations..

3.1.1 Suprenovae Observations

The supernova explosion can be triggered in two ways. In both ways, it is gravity that gives a Supernovae its energy.

1. By the abrupt re-ignition of nuclear fusion in a compact star. The compact star may accumulate sufficient material from it's surroundings, either by a merger or through accretion, to raise its core temperature and ignite nuclear fusion, completely disrupting the star.
2. By the collapse of the core of the massive star. Mass flows into the core of the star by the continued formation of iron from nuclear fusion. Once the core has gained so much mass that it cannot withstand its own weight (gravity), the core implodes. If the mass of the star core is higher then the Chandrasekhar limit (1.38M),then even neutrons fail to stop the implosion, thus turning the implosion into an explosion.

Why Type Ia supernovae?

Type Ia supernovae are among the brightest objects in the universe and they are all almost the same brightness with the difference that can be standardized to less than 10 percent. They are excellent standard candles for measuring the expansion history of the universe. Thus the supernovae's apparent brightness shows how far away it is and how much light takes time to travel, how far back in time it exploded.
The procedure is straight forward; by comparing the brightness to redshift for numerous Type Ia supernovae, from nearby to very distant, an observer can tell how the rate of expansion of universe has changed over time. Brighter supernovae of this type wax and wave more slowly than the fainter ones.
The Type Ia supernovae is used for observation due to following reasons:

1. They are found in all types of galaxies.

2. They show strong emission of Si(II) ($\lambda = 6150\dot{A}$) unlike other supernovae which emit the more general hydrogen lines in majority.

3. They are most likely the explosion of white dwarf.

The last point requires elaboration. White dwarfs which form the final evolutionary stage of less massive stars no longer maintain their internal pressure by nuclear fusion. For $M \sim M_{CH}$, the degeneracy pressure can no longer balance the gravitational force. As we have a sharp limit for the white dwarf stars, we can say that all Type Ia supernovae has formed under homogeneous circumstances and therefore their luminosities are nearly the same.

Estimation of luminosity distance

Empty universe would expand at constant rate $\ddot{a} = 0$. The luminosity distance in such a universe is larger than in any other universe with a vanishing cosmological constant. The luminosity distance can only be increased by assuming expansion has acceleration over time. It is possible only if $\Omega_\Lambda > 0$. SNIa become brighter than would be in an empty universe. At these high redshift, the matter density dominates the universe, proceeding as $(1 + z)^3$ in contrast to constant vacuum energy. As we know from eqns (1.40) and

(1.43)

$$r_s = \int_0^z d_H(z)dz \tag{3.2}$$

and

$$d_L(z) = r_s(1+z) = (1+z)\int_0^z d_H(z)dz \tag{3.3}$$

By definition of hubble distance, we know the expression

$$d_H(z) = H_0^{-1}\left(\Omega_r(1+z)^4 + \Omega_n(1+z)^3 + \Omega_\Lambda + (1-\Omega)(1+z)^2\right)^{-1/2} \tag{3.4}$$

So far we have used the value of c = 1. But now for data analysis we have to convert the equation of d_L in the units of distance.So,the above equation can be written as

$$d_L(z) = \frac{c}{H_0}(1+z)\int_0^z d_h(z)dz \tag{3.5}$$

Where,

$$d_H(z) = H_0^{-1}d_h(z) \tag{3.6}$$

The units of c is Kms^{-1} and the units of H_0 is $Kms^{-1}Mpc^{-1}$.So, in the above equation the units of d_L is Mpc. But from Eq.(1.24),the unit of d_L must be in parsec. So, taking all factors in account and putting value of $c = 3\times10^5\mathrm{Km}s^{-1}$ and $H_0 = 70kms^{-1}Mpc^{-1}$, we get

$$d_L = 5\times log_{10}(4285.7(1+z)\int_0^z d_h(z)dz) \tag{3.7}$$

The data comprises of the above derived quantity for the given redshift. So, for the various cosmological models, distance modulus is calculated for the particular redshift given in the data and then fit it with observation by χ^2 minimization technique.

3.1.2 Baryonic Acoustic Oscillation (BAO) Data

Before the recombination epoch, baryons are tightly coupled to photons. So, sound waves oscillations will be present in the baryon perturbations. These perturbations are detected as baryonic acoustic oscillation peak by the large-scale correlation function measured from a spectroscopic sample of luminous red galaxies from Sloan Digital Sky Survey(SDSS). The detection of BAOs(Baryonic Acoustic Oscillations) provides another independent tech-

nique for probing dark energy.
The data (essentially contains 6 data points)consists of the effective distance parameter(d_z) and acoustic parameter(A(z)) at particular redshift z and the error associated with the measurement of these two quantities. In the next section, only A(z) is used for data analysis.

Background

The sound horizon at which baryons were released from the Compton drag of photons determines the location of the baryon acoustic oscillation peak length scale. This epoch called the drag epoch, occurs at the redshift z_d and the length scale is

$$r_s(z_d) = \int_0^{\eta_{drag}} c_s(\eta) d\eta \tag{3.8}$$

Where c_s is the speed of sound and η is the conformal time. The drag epoch is not the same as the recombination epoch when photons are released from electrons. The observed angular and redshift distribution of galaxies is determined by the power spectrum P($k_\parallel, k_\perp$); where $k_\parallel$and $k_\perp$ are the components of wavenumbers parallel and perpendicular to the line of sight respectively. Consider two ratios

$$\theta_s^2(z) = \frac{r_s(z_d)}{(1+z)d_A(z)}, \qquad \delta z_s(z) = \frac{r_s(z_d)H(z)}{c} \tag{3.9}$$

The first ratio corresponds to the angle distribution orthogonal to the line of sight and the second one corresponds to oscillation along the line of sight. Most current BAO observations cannot measure these two ratios independently but form a spherically averaged spectrum. It is possible to determine the quantity

$$\Big[\theta_s(z)^2 \delta z_s(z)\Big]^{1/3} = \frac{r_s(z_d)}{\Big[(1+z)^2 d_A^2(z) c/H(z)\Big]^{1/3}} \tag{3.10}$$

Effective distance ratio is defined as the denominator of the right hand side of the above equation.

$$D_v(z) = \Big[\tfrac{(1+z)^2 d_A^2(z) c}{H(z)}\Big]^{1/3} \tag{3.11}$$

The effective distance ratio is the central term in BAO measurement. The observations measures two parameters both of which includes $D_v(z)$. The one refers to the Radius of BAO defined as

$$r_{BAO} = \frac{r_s(z_d)}{D_v(z)} \tag{3.12}$$

The another is called acoustic parameter defined mathematically as

$$A(z) = \frac{100 D_v(z)\sqrt{\Omega_m h^2}}{cz} \tag{3.13}$$

Using Eq.(2.45), the angular diameter distance is defined as

$$d_A(z) = \frac{\int_0^z d_H(z)dz}{(1+z)} \tag{3.14}$$

As $d_A(z)$ is used in the units of Mpc, The value of angular diameter distance must be multiply by the factor c/H_0. The value of H_0 is taken as 70 $Kms^{-1}Mpc^{-1}$ for the contraining the parameter except in the last section, where the effect variation of h on parameters is also analysed. From Eq.(2.46), the value of $d_H(z)$ is obtained and will be changed according to the models considered.

$$d_H(z) = H_0^{-1}\left(\Omega_n(1+z)^3 + \Omega_v(1+z)^{3(1+w)}\right)^{-1/2} \tag{3.15}$$

The value of H(z) will be obtained from Eq.(1.3) and defined as

$$H(t) = H_0\left(\Omega_n(1+z)^3 + \Omega_v(1+z)^{3(1+w)} + (\Omega-1)(1+z)^2\right)^{1/2} \tag{3.16}$$

3.1.3 Hubble Parameter Measurement (H(z)) data

The value of Hubble Parameter is now available and can be used to constrain the cosmological parameters. In the standard picture of cosmology, Dark energy plays a significant role in current accelerating cosmological expansion but plays less significant role in past when non-relativistic matter dominated. The data comprises of 28 independent measurements of Hubble parame-

ter(H(z)) and is available at the redshifts in the range $0.07 \geq z \geq 2.3$. The data set essentially comprise of Hubble parameter $H(z_i)$ at the redshift z_i and the error associated with the Hubble parameter $\sigma_{H(z_i)}$
The task is to establish that the three models of dark energy are good fit to data and the data provide tight constraints on the parameters given in the models. Finally, an attempt is made to tighten the constrain by varying the value of h.

3.2 Scalar Field Models of Dark Energy

The cosmological constant corresponds to a fluid having constant value of equation of state (w=-1). The observations which constrain the value of w close to -1 say little about the time evolution of w. Therefore, we consider a situation in which equation of state of dark energy changes with time. Scalar fields arise in particle physics including string theory and can act as candidate of dark energy. Various scalar field models have proposed so far.

3.2.1 Quintessence

It is described by an ordinary scalar field ϕ minimally coupled to gravity. The action for quintessence is given by

$$S = \int d^4x\sqrt{-g}\left(-\tfrac{1}{2}(\nabla\phi)^2 - V(\phi)\right) \tag{3.17}$$

Where

$$(\nabla\phi)^2 = g^{\nu\mu}\partial_\nu\phi\partial_\mu\phi \tag{3.18}$$

and $V(\phi)$ is the potential of the field. In the flat FRW spacetime, the variation of the action with respect to ϕ is given by

$$\ddot{\phi} + 3H\dot{\phi} + \frac{dV}{d\phi} = 0 \tag{3.19}$$

The energy momentum tensor is derived by varying the action in terms of $g^{\mu\nu}$.

$$T_{\nu\mu} = \frac{2\partial S}{\sqrt{-g}\partial g^{\nu\mu}} \tag{3.20}$$

and

$$\partial(\sqrt{-g}) = -\frac{1}{2}\sqrt{-g}g_{\nu\mu}\partial g^{\nu\mu} \tag{3.21}$$

In the flat Friedmann background, we obtain the energy density and pressure density.

$$H^2 = \frac{8\pi G}{3}\left(-\tfrac{1}{2}(\nabla\phi)^2 + V(\phi)\right) \tag{3.22}$$

$$\frac{\ddot{a}}{a} = -\frac{8\pi G}{3}\left((\nabla\phi)^2 - V(\phi)\right) \tag{3.23}$$

for $\nabla\phi)^2 < V(\phi)$, universe accelerates. This means that flat potential is required to give rise to an accelerated expansion. The equation of state for the field ϕ is given by

$$w_\phi = \frac{p}{\rho} = \frac{(\nabla\phi)^2 - 2V(\phi)}{(\nabla\phi)^2 + 2V(\phi)} \tag{3.24}$$

In order to determine the form of the potential $V(\phi)$, we can derive a scalar field potential that give rise to power law expansion

$$a \propto t^p \tag{3.25}$$

The accelerated expansion occurs for $p > 1$. The potential giving the power-law expansion corresponds to

$$V(\phi) = V_0 exp(\alpha\phi) \tag{3.26}$$

The exponential potential possess cosmological scaling solutions in which the field energy density (ρ_ϕ) is propotional to fluid energy density (ρ_m). The original quintessence models are described by power law type potential

$$V(\phi) = \frac{V_0}{\phi} \tag{3.27}$$

There are several form of potential available which is essentially the permutation of the two forms discussed above. The forms taken here for the analysis is

- $V(\phi) = \frac{M^{4+n}}{\phi^n}$

- $V(\phi) = \frac{M^{4+n} exp(\alpha\phi^2)}{\phi^n}$

Where n is an integer goes from -3 to +3, $\kappa^2 = 8\pi G$ and $M^{-2} = \kappa^2$.

Where w_i is the initial value of w given to solve the equation analytically. For solving the equations 3.23 and 3.26, we used the substitutions

$$t_0 = xH_0 \qquad \frac{\phi}{m_p} = \psi \tag{3.28}$$

with initial conditions

$$\dot{\phi}_0 = \sqrt{3(1-\Omega_m)(1+w_i)} \qquad and \qquad \phi_0 = 1.0 \tag{3.29}$$

So, the equations for the exponential potential become

$$\psi'' + \frac{3y'\psi'^2}{y} + \frac{V_0 exp(\alpha\psi^2)}{\psi^{n-1}} \left(2\alpha - \tfrac{n}{\psi^2}\right) \tag{3.30}$$

$$(\frac{y'}{y})^2 = \Omega y^{-3} + \frac{\psi'^2}{6} + \frac{V_0}{3\psi^n} \tag{3.31}$$

Where

$$V_0 = \frac{M^2}{H_0^2} = \frac{3(1-w_i)(1-\Omega_m)}{2} \tag{3.32}$$

These coupled equations are solved analytically and the value of ψ and $\dot{\psi}$. These values are used to determine equation of state parameter w.

$$w = \frac{\psi'^2 - \frac{2V_0 exp(\alpha^2)}{\psi^n}}{\psi'^2 + \frac{2V_0 exp(\alpha^2)}{\psi^n}} \tag{3.33}$$

Likewise for the inverse potential, the equation to be solved is

$$\psi'' + \frac{3y'\psi'^2}{y} + \frac{V_0 n}{\psi^{n+1}} \tag{3.34}$$

$$(\frac{y'}{y})^2 = \Omega y^{-3} + \frac{\psi'^2}{6} + \frac{V_0}{3\psi^n} \tag{3.35}$$

The value of w to be obtained will be

$$w = \frac{\psi'^2 - \frac{2V_0}{\psi^n}}{\psi'^2 + \frac{2V_0}{\psi^n}} \tag{3.36}$$

We have the value of w. All we need to do now is use these values in compute the quantities

- Distance modulus(SNIa) $d_L = (1+z)\int_0^z d_H(z)dz$
- Angular Diameter Distance (BAO)$d_A = \frac{d_L}{(1+z)^2}$
- Hubble parameter H(z) = $d_H(z)^{-1}$
- $d_H(z) = (\Omega_m(1+z)^3 + \Omega_\lambda)^{-1/2}$

for the redshift given in the data sets and compute the maximum likelihood (χ^2) for those values.

Chapter 4

Observational Constraints

In this chapter, We analyse the three data sets one at a time for the different models of cosmology. The parameters to be constrained are matter density (Ω_m), vaccum energy density (Ω_λ), curvature density (Ω_k), equation of state (w) and w'(used in the parametrization of w). We also do a combined analysis of different data sets.
Finally we use the particle physics scalar field model (Quintessence) to determine w.

4.1 Cosmological Constant Model

For Supernovae data, we have the value of d_L with constant value of matter density. We have the data set comprises of redshift, $d_m(d_m = 5logd_L - 5)$ and uncertainty associated with each data point. For those given redshifts, we compute theoretically, the d_m and fit it with the χ^2 minimization method. Then we plot χ^2 and Ω_{NR} and find for which value of matter density is the χ^2 minimum. Fig.5.1 represents the χ^2 v/s Ω_{NR} plot and we find that the value of χ^2 is minimum at $\Omega = 0.27$.

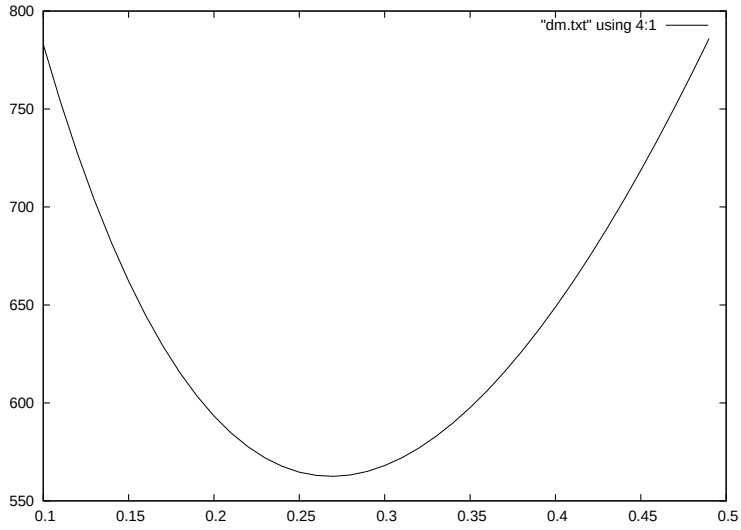

Figure 4.1: χ^2 v/s Ω_n for flat cosmology with the model $\Omega_n + \Omega_v + \Omega_R = \Omega$ for Supernovae data

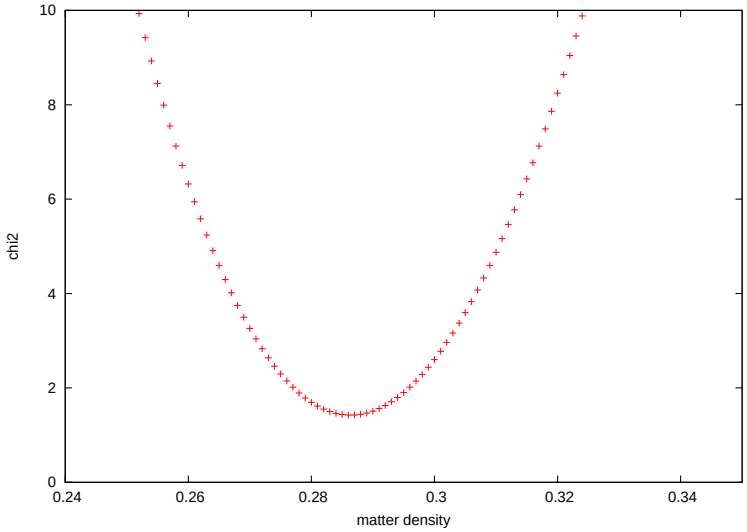

Figure 4.2: χ^2 v/s Ω_n for flat cosmology with the model $\Omega_n + \Omega_v = \Omega$ for BAO data

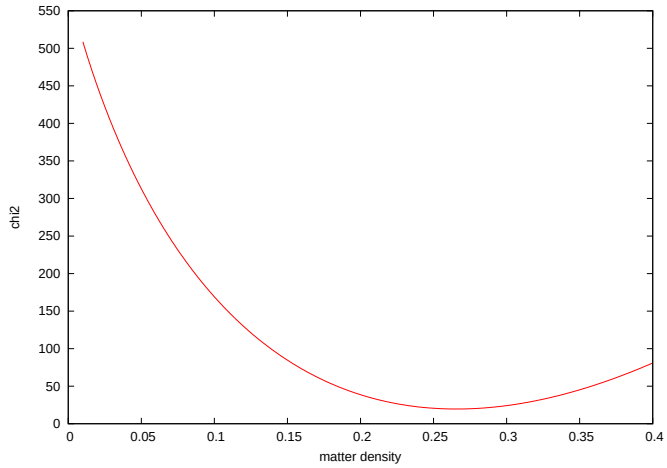

Figure 4.3: χ^2 v/s Ω_n for flat cosmology with the model $\Omega_n + \Omega_v = \Omega$ for H(z) data

For BAO data, the minimum χ^2 value of 1.51 is obtained for $\Omega_n = 0.286$ (Fig.5.2).
The model to be analysed is the Definition of H(z) given by Eq.(4.19) in the previous section with value of w taken to be -1 and the value of $\Omega(= \Omega_v + \Omega_n)$ be 1. The equation to be analysed is

$$H(t) = H_0 \left[\Omega_{nr}(1+z)^3 + \Omega_v\right]^{1/2} \tag{4.1}$$

The minimum χ^2 value of 19.588 is obtained at $\Omega_n = 0.266$. Fig.5.3 represents the behaviour of χ^2 with Ω_n.

4.2 Cosmological Models with w $= p/\rho$ where $w \neq -1$

In the previous section, there is only one parameter i.e. Ω_{NR} within the range 0.1-0.5 and the value of w to be -1.0 so that there is no z dependence in the second term of Eq.(2.3). As the universe evolves, the contribution of radiation diminishes gradually. As the value of redshift we are considering is very low (0.05-1.414), we can ignore the radiation completely. In addition to

this, we are considering the flat universe i.e.

$$(\Omega = 1 = \Omega_n + \Omega_v) \tag{4.2}$$

and for w = -1

$$\Omega_v = \Omega_\lambda \tag{4.3}$$

Now, the value of w changes within the range -1.5 to -0.6. The equation now to be solved for supernovae data is

$$d_L(z) = r_s(1+z) = (1+z)\int_0^z d_H(z)dz \tag{4.4}$$

The value of $d_H(z)$ will be

$$d_H(z) = H_0^{-1}\left(\Omega_n(1+z)^3 + \Omega_v(1+z)^{3(1+w)}\right)^{-1/2} \tag{4.5}$$

For this equation, we have calculated the χ^2 for every combination of Ω_n and w. The minimum χ^2 value of 562.344 is obtained for

$$a = 0.29 \qquad \& \qquad w = -1.05 \tag{4.6}$$

We represent our result here in Fig.4.4 in the form of contours of 1σ, 2σ and 3σ confidence intervals in the value of χ^2 in Ω_n-w plane.

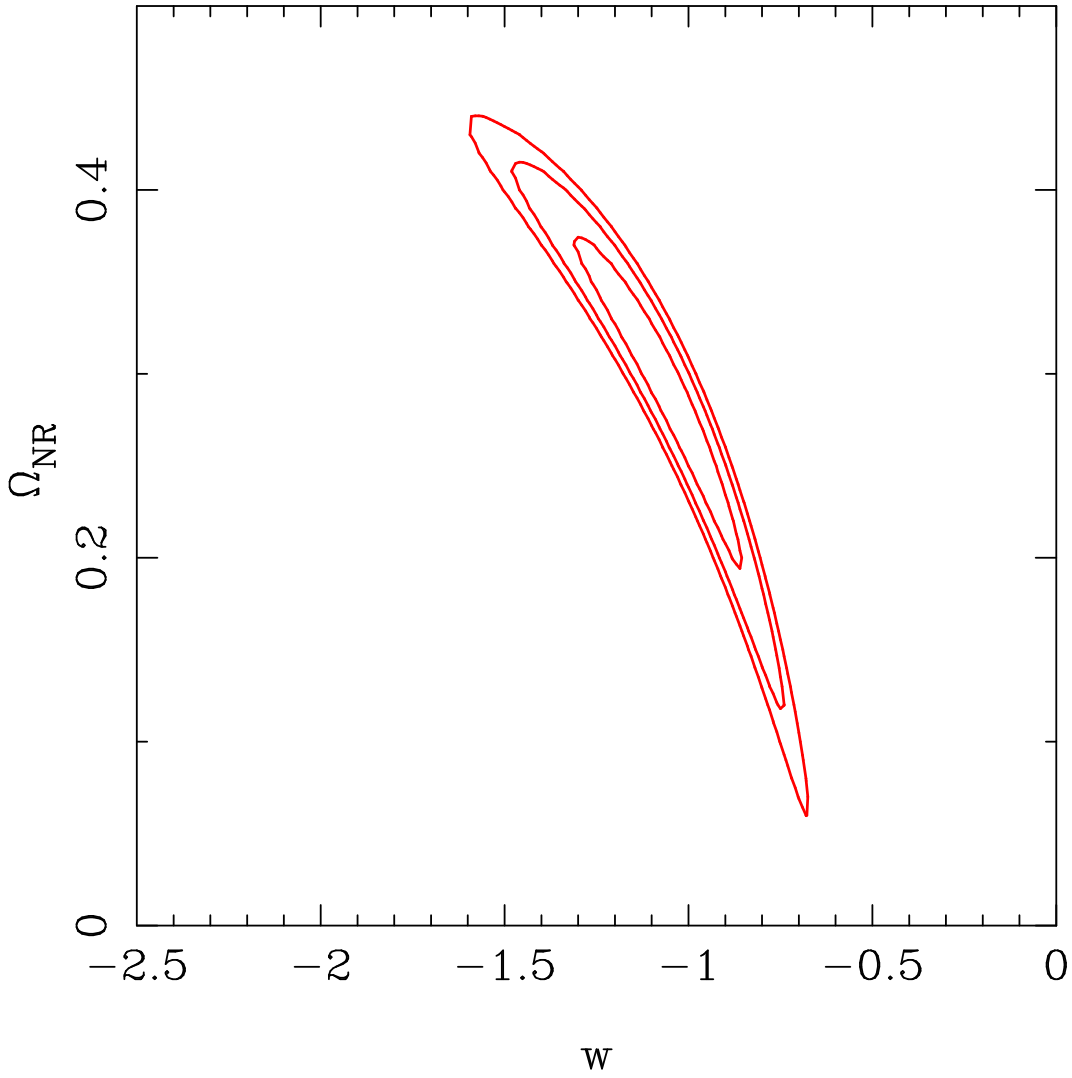

Figure 4.4: 1σ, 2σ and 3σ contours in w-Ω_n plane for Supernovae data.

The minimum value of 0.95 for χ^2 is obtained for $\Omega_n = 0.268$ and w = -1.184. Fig.4.5 represents the 1-σ, 2σ contours in Ω_n-w plane.

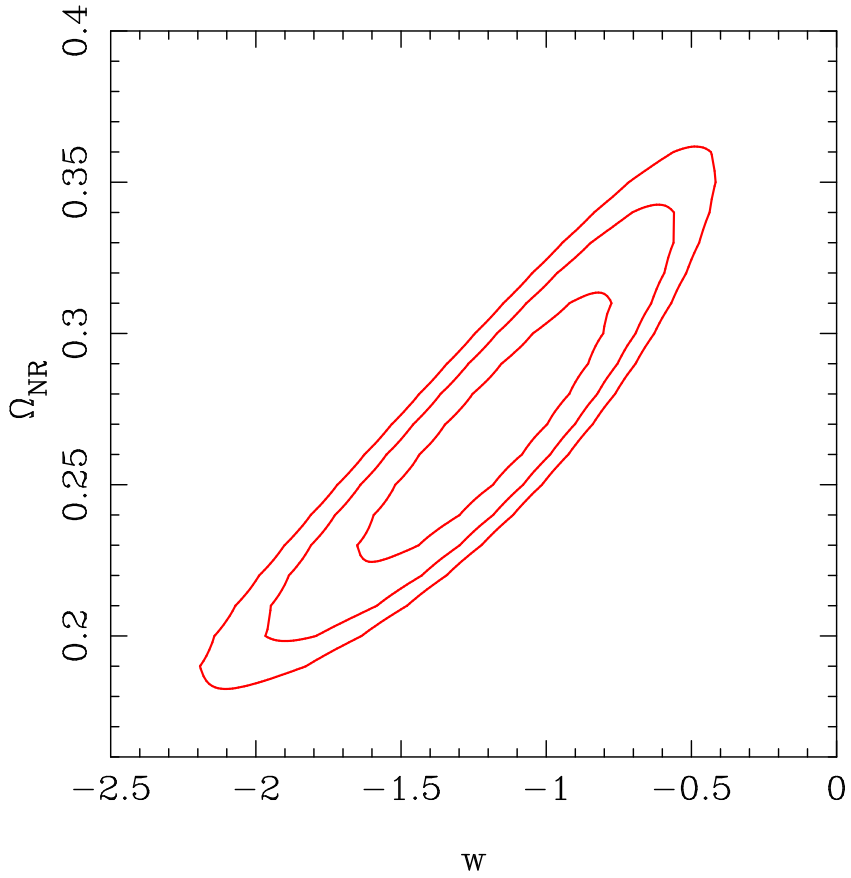

Figure 4.5: 1σ, 2σ and 3σ contours in w-Ω_n plane for BAO data set.

For H(z) data set, the minimum value of 19.30 is obtained for χ^2 is obtained for $\Omega_{nr} = 0.276$ and w=-1.06. Fig.4.6 represents the 1σ, 2σ and 3σ contours in Ω_n-w plane.

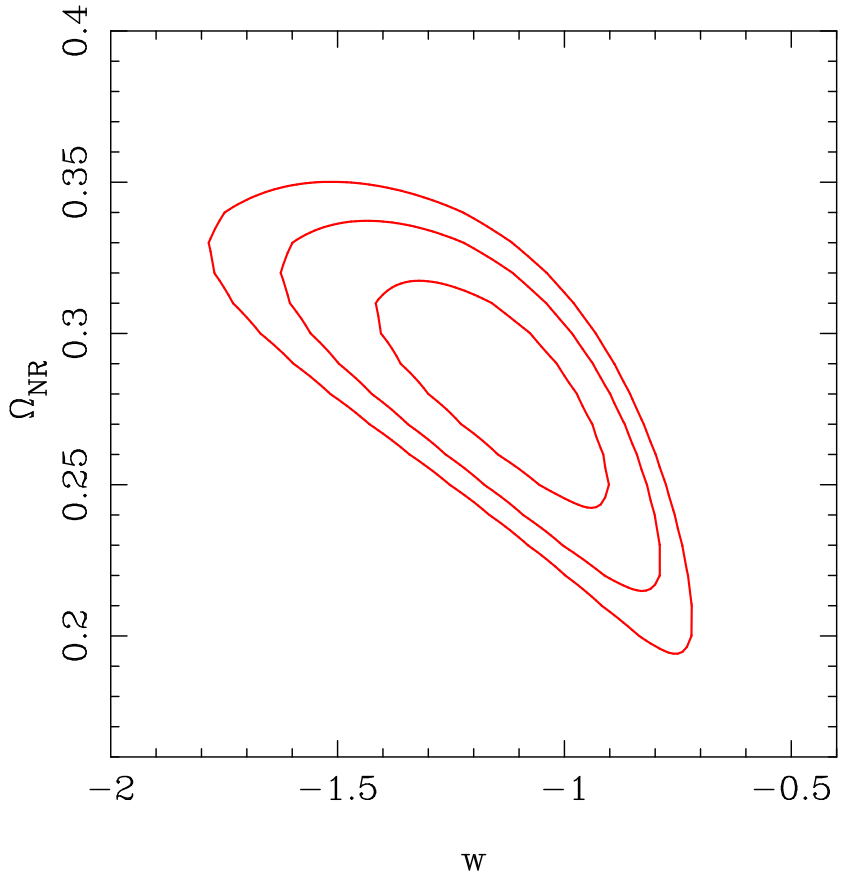

Figure 4.6: 1σ, 2σ and 3σ contours in w-Ω_n plane for H(z) data.

4.3 Modification in the value of w

The definition of state parameter w comes from the equation of state

$$p = w\rho \tag{4.7}$$

Considering the existing models, it can be inferred that w in general varies with redshift. One can generalise the models to the models with varying value of state parameter w(z). Since a function is equivalent to an infinite set of numbers (defined by a Taylor-Laurent series coefficients), it is clearly not possible to constrain the form of an arbitrary function w(z) using finite number of observations. This problem is solved by parameterizing the state

parameter by a finite number of parameters and constraining these parameters by observations.
Here, we have used two parametrization

$$w(z) = w_0 + w_1 \frac{z}{(1+z)^p}; \qquad p = 1, 2 \tag{4.8}$$

They are chosen so that the redshift behavior is completely different in both the parametrization. For p = 1, the asymptotic value of w(z); $w(\infty) = w_0 + w'(z=0)$ and for p = 2, $w(\infty) = w_0$. But for both p = 1,2; the present value is $w(0) = w_0$.
For p=1, the value of d_H(z) to be used is

$$d_H(z) = H_0^{-1} \left(\Omega_n (1+z)^3 + \Omega_v (1+z)^{3(1+w_0+w'(z=0)\frac{z}{1+z})} \right)^{-1/2} \tag{4.9}$$

For this equation, we calculated the χ^2 for every combination of matter density, w_0 and w_1. The ranges of Ω_n is same as that in previous calculations and the same range is used for both w_0 and $w'(z=0)$.

We represent the result in the form of contours of 1σ, 2σ and 3σ confidence intervals in the value of χ^2 in $\Omega_n - w_0$ and $w_0 - w'(z=0)$plane. For p=2, the value of d_H(z) to be used is

$$d_H(z) = H_0^{-1} \{ \Omega_n (1+z)^3 + \Omega_v (1+z)^{3(1+w_0+w'(z=0)\frac{z}{(1+z)^2})} \}^{-1/2} \tag{4.10}$$

For this equation we calculated the χ^2 for every combination of matter density, w_0 and w_1. The ranges of Ω_n is same as that in previous calculation. For the supernovae data, the minimum χ^2 value of 562.56 for p=1 is obtained for

$$\Omega_n = 0.35; \qquad w_0 = -1.12; \qquad w'(z=0) = -0.49 \tag{4.11}$$

For p=2, The minimum χ^2 value of 562.78 is obtained for

$$\Omega_n = 0.38; \qquad w_0 = -1.16; \qquad w'(z=0) = -0.6 \tag{4.12}$$

We represent the result in the form of contours of 1σ and 2σ confidence intervals in the value of χ^2 in $\Omega_n - w_0$ and $w_0 - w'(z=0)$ plane. Fig.5.7

represents the 1σ, 2σ and 3σ contours in $\Omega_n - w$ plane and $w_0 - w_1$ plane for both values of p for supernovae data. For BAO data, the minimum value of χ^2 is 0.8684, is obtained for p=1 corresponding to

$$\Omega_n = 0.291; \qquad w_0 = -0.66; \qquad w'(z=0) = -1.35 \tag{4.13}$$

Fig.5.8 represents the 1-σ, 2σ contours in $\Omega_n - w$ plane. Fig.5.8 represents the 1σ, 2σ and 3σ contours in $w_0 - w_1$ plane. For p=2, the minimum value of χ^2 of 0.85 is obtained corresponding to

$$\Omega_n = 0.281; \qquad w_0 = -0.81; \qquad w'(z=0) = -1.5 \tag{4.14}$$

Fig.5.8 represents the 1σ, 2σ and 3σ contours in Ω_n-w plane and $w_0 - w_1$ plane for both values of p for BAO data. For H(z) data, the equation to be used for p=1 is

$$H(t) = H_0 \left(\Omega_{nr}(1+z)^3 + \Omega_v (1+z)^{3(1+(w_0+w_1 z/(1+z)))}\right)^{1/2} \tag{4.15}$$

The minimum χ^2 value of 19.32 is obtained corresponding to Ω_n=0.289, w_0=-0.97 and w_1 = -0.49. For p=2, the equation used is

$$H(t) = H_0 \left(\Omega_{nr}(1+z)^3 + \Omega_v (1+z)^{3(1+(w_0+w_1 z/(1+z)^2))}\right)^{1/2} \tag{4.16}$$

The minimum value 18.99 of χ^2 is obtained for Ω_n=0.282, w_0=-0.82 and w_1 = -1.39. Fig.5.9 represents the 1σ, 2σ and 3σ contours in $\Omega_n - w$ plane and $w_0 - w_1$ plane for both values of p for H(z) data.

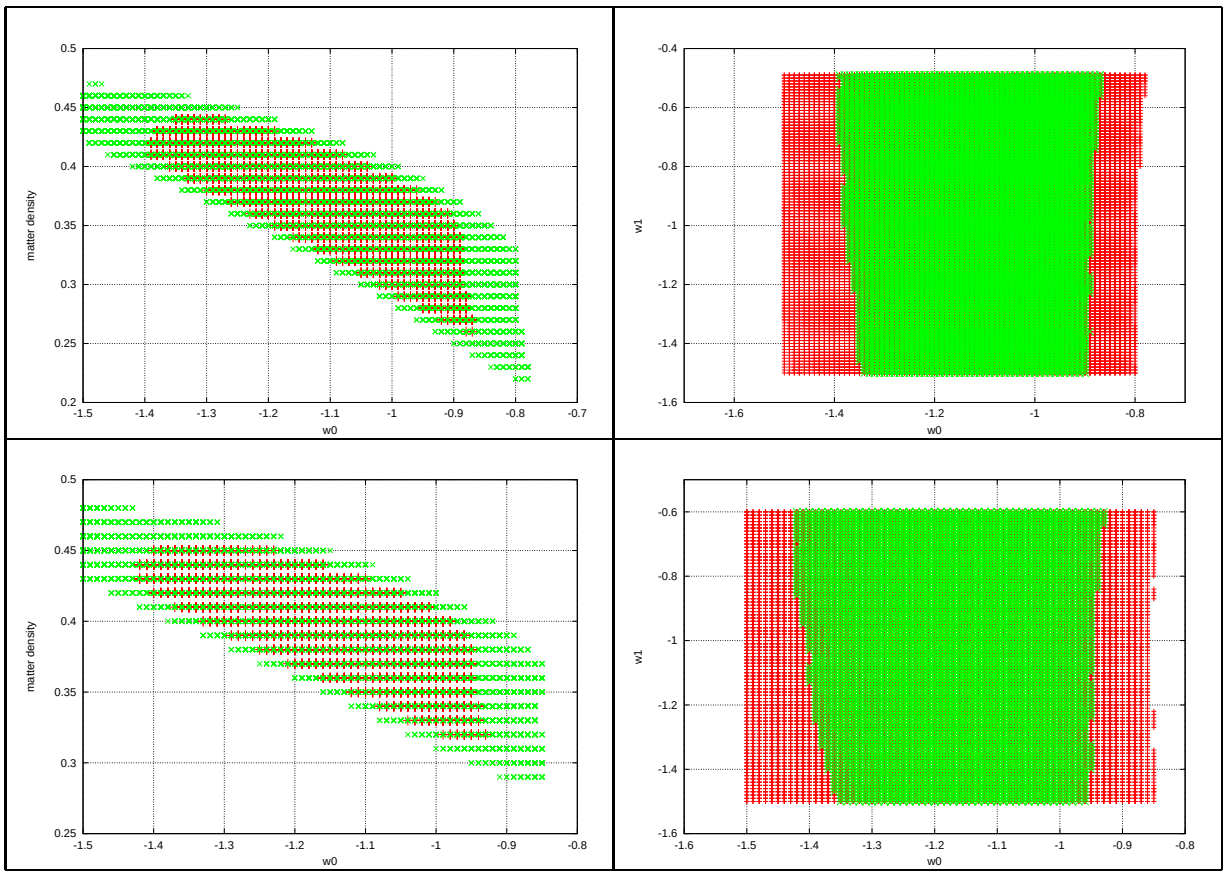

Figure 4.7: Contours in Ω_{nr}-w plane and w-w' plane obtained by analysis of supernovae data. The upper figures correspond to p=1 value and lower figures to that of p=2.

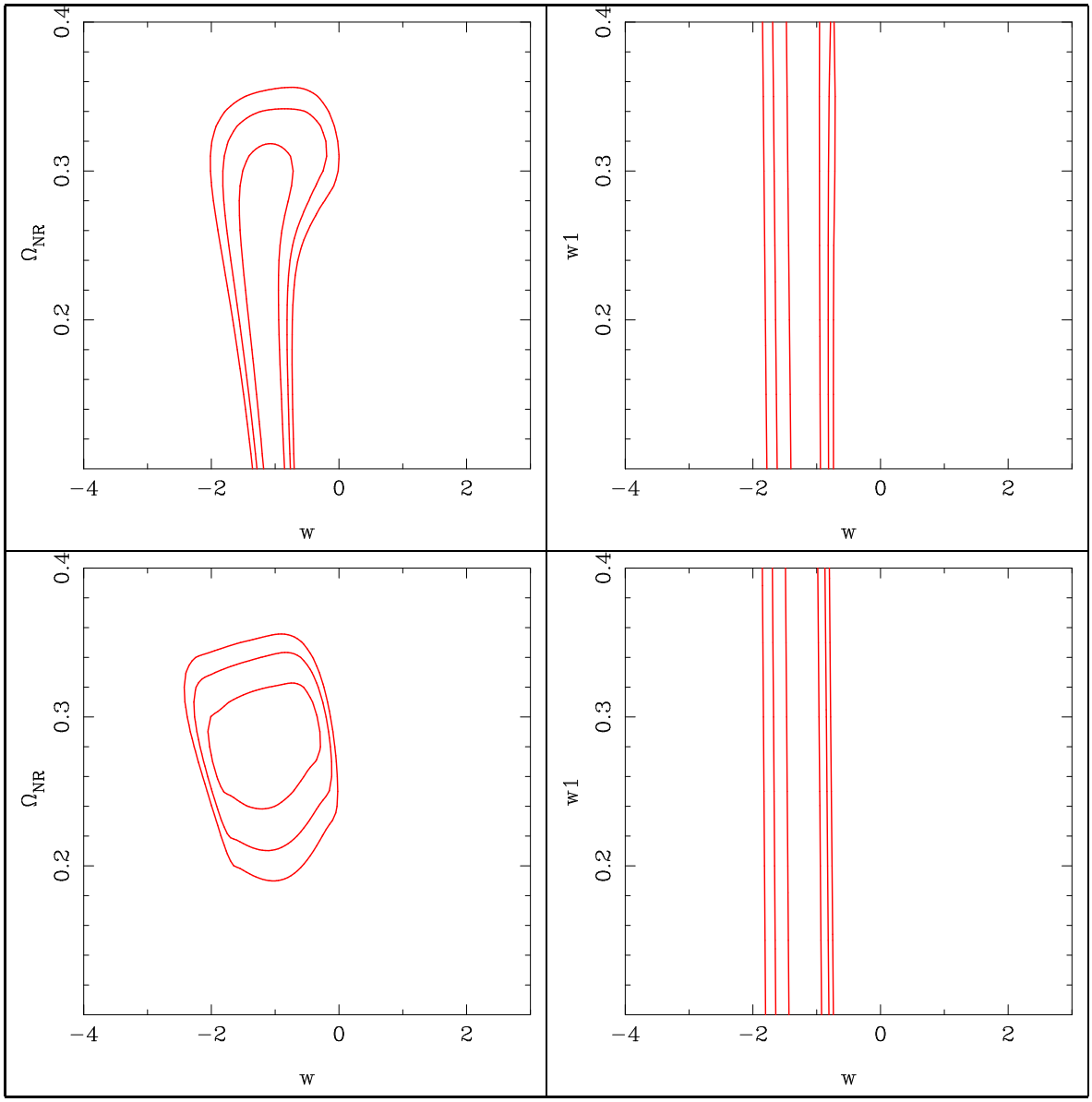

Figure 4.9: Contours in Ω_{nr}-w plane and w-w' plane obtained by analysis of H(z) data. The upper figures correspond to p=1 value and lower figures to that of p=2.

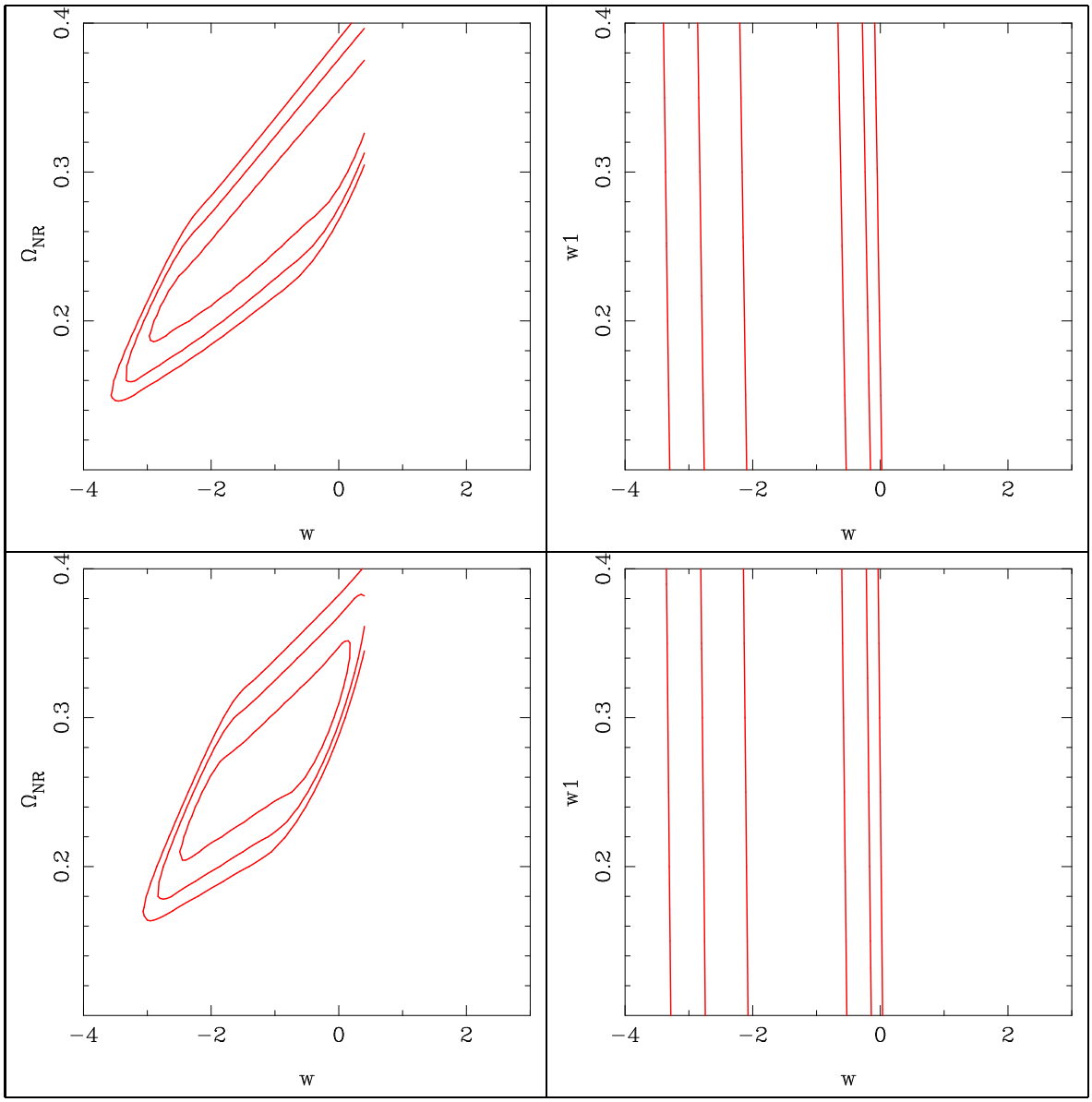

Figure 4.8: Contours in Ω_{nr}-w plane and w-w' plane obtained by analysis of BAO data. The upper figures correspond to p=1 value and lower figures to that of p=2.

4.4 Open and Closed Universe

As discussed earlier, Luminosity distance is defined as

$$d_L = a_0 r_s (1+z) \tag{4.17}$$

Where a_0 is the scale factor at t=t_0, r_s is the distance of radiation and z is the redshift. From equation 2.39, we can write

$$\frac{1}{a_0}\int_0^z d_H(z)dz = S_k^{-1}(r_s) \tag{4.18}$$

For k = -1, $s_k^{-1}x = sinh^{-1}x$, So the equation takes the form

$$\frac{1}{a_0}\int_0^z d_H(z)dz = sinh^{-1}r_s \tag{4.19}$$

Rearranging it, we get

$$r_s = sinh\left(\frac{1}{a_0}\int_0^z d_H(z)dz\right) \tag{4.20}$$

Solving Eq.2.16 at t=t_0, we get

$$a_0 = H_0^{-1}(|\Omega - 1|)^{-1/2}; \frac{k}{a_0^2} = H_0^2(\Omega - 1) \tag{4.21}$$

It is clear that k = -1, 0 or 1,depending on whether $\Omega < 1$, $\Omega = 1$ or $\Omega > 1$ respectively. Putting value of a_0 and d_H(z) from Eq.2.46, we get

$$d_L = H_0^{-1}(1-\Omega)^{-1/2} Sinh(H_0(1-\Omega)^{1/2} H_0^{-1}\int_0^z d_h(z)dz) \tag{4.22}$$

Which reduces to

$$d_L = H_0^{-1}(1-\Omega)^{-1/2} Sinh((1-\Omega)^{1/2}\int_0^z d_h(z)dz) \tag{4.23}$$

Where

$$H_0^{-1} d_h(z) = d_H(z) \tag{4.24}$$

For K=1, $S_k^{-1}x = sin^{-1}x$ and $\Omega > 1$. So, the above equation modifies to

$$d_L = H_0^{-1}(\Omega - 1)^{-1/2} Sin((\Omega - 1)^{1/2} \int_0^z d_h(z)dz) \tag{4.25}$$

Solving this numerically, the value of d_h(z) is taken to be

$$d_h(z) = [\Omega_n(1+z)^3 + \Omega_v + (1-\Omega)(1+z)^2]^{-1/2} \tag{4.26}$$

The ranges for Ω_n, Ω_v and Ω is taken to be (0 - 1.0), (0 - 1.0) and (0.25 - 1.75) respectively. Here, both the matter density and vaccum density are independent.
For the supernovae data, the minimum value 562.38 of χ^2 is obtained for

$$\Omega_n = 0.29, \qquad \Omega_v = 0.76 \qquad \Omega = 1.05 \tag{4.27}$$

For BAO data, the minimum value of 1.42 of χ^2 is obtained corresponding to

$$\Omega_n = 0.39; \qquad \Omega_v = 0.96; \qquad \Omega = 0.99 \tag{4.28}$$

For H(z) data, the minimum value of 19.52 for χ^2 is obtained corresponding to

$$\Omega_n = 0.27 \qquad \Omega_v = 0.71 \qquad \Omega = 0.999 \tag{4.29}$$

Fig.5.11 represents the constraints obtained by analysing the three data sets. The 1σ, 2σ and 3σ contours are in $\Omega_{nr} - \Omega_\Lambda$ plane and $\Omega_{nr} - k$ plane.

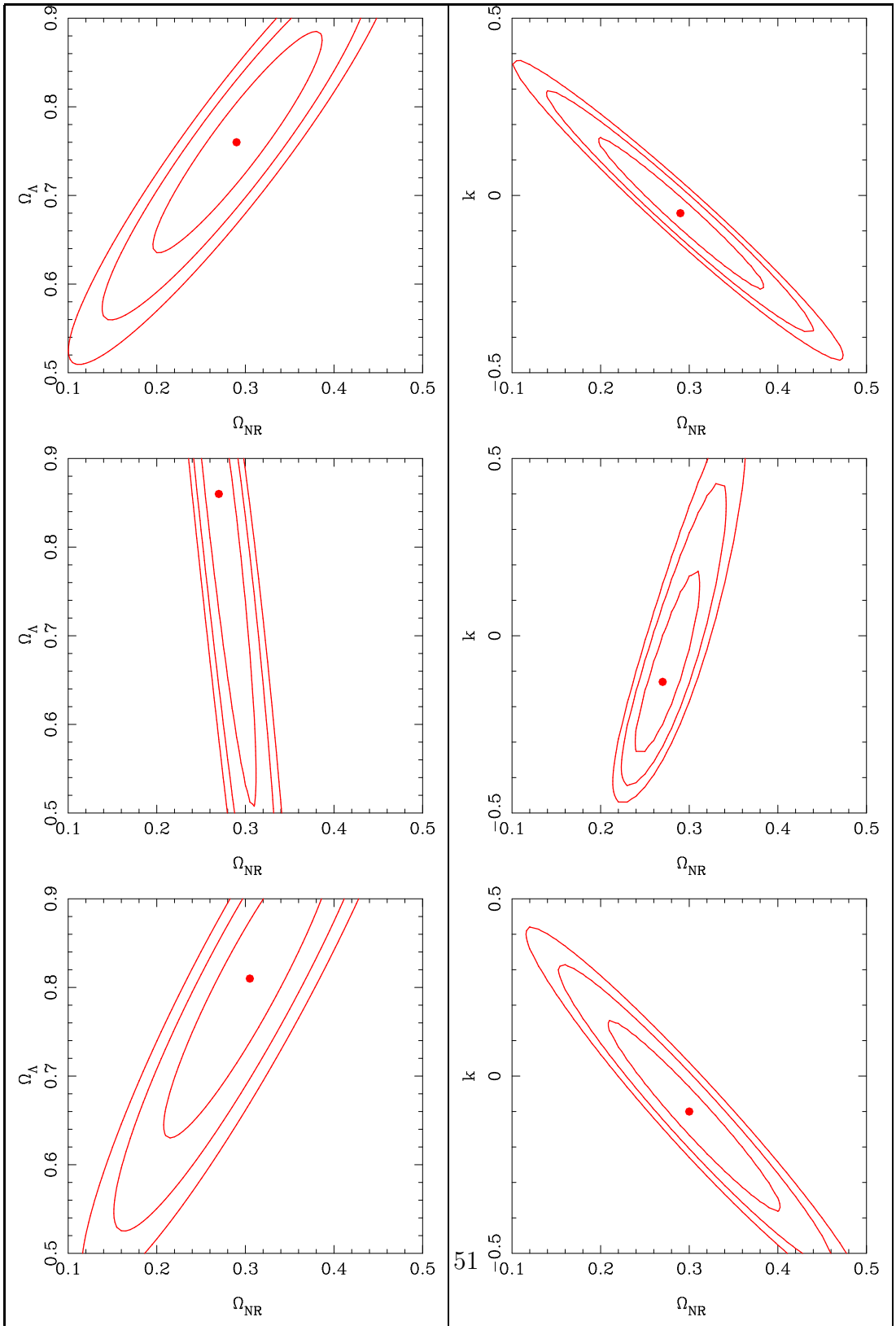

Figure 4.10: Constraints for non-flat universe. First column represents constraints in Ω_{nr}-Ω_Λ plane and second corresponds to that in Ω_{nr}-k plane. The first, second and third row corresponds to constraints obtained by the analysis of Supernovae, BAO and H(z) data respectively.

4.5 Dark Energy Density as a Function of Redshift

As discussed earlier, The total density of the universe consists of matter density, vacuum density and radiation density

$$\rho_{total} = \rho_n + \rho_r + \rho_{DE} \tag{4.30}$$

The equation used to understand the effect of dark energy on other parameters is

$$\rho_{DE}(z) = \Omega_v(1+z)^{3(1+w)} \tag{4.31}$$

Initially,the ρ_{DE} is found for fixed value of Ω_v (0.3) and constant w (-1.5, -1, -0.5). From the plot, we can infer that for w = -1, dark energy doesn't vary with redshift.

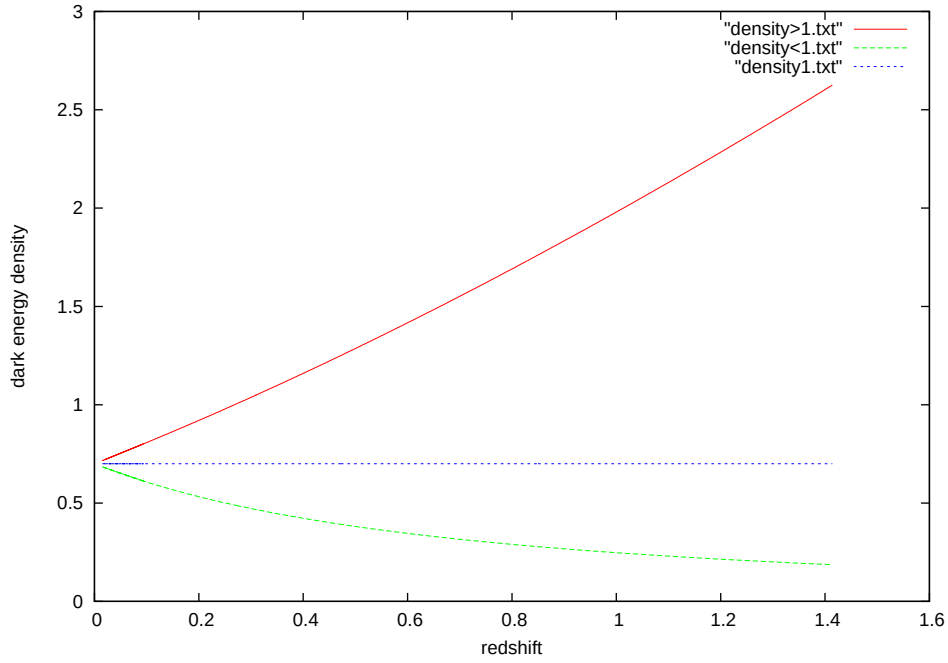

Figure 4.11: $\rho(z)$ v/s z for constant w (-1.5,-1,-0.5)

Let's consider the flat universe. Now, in order to vary the remaining

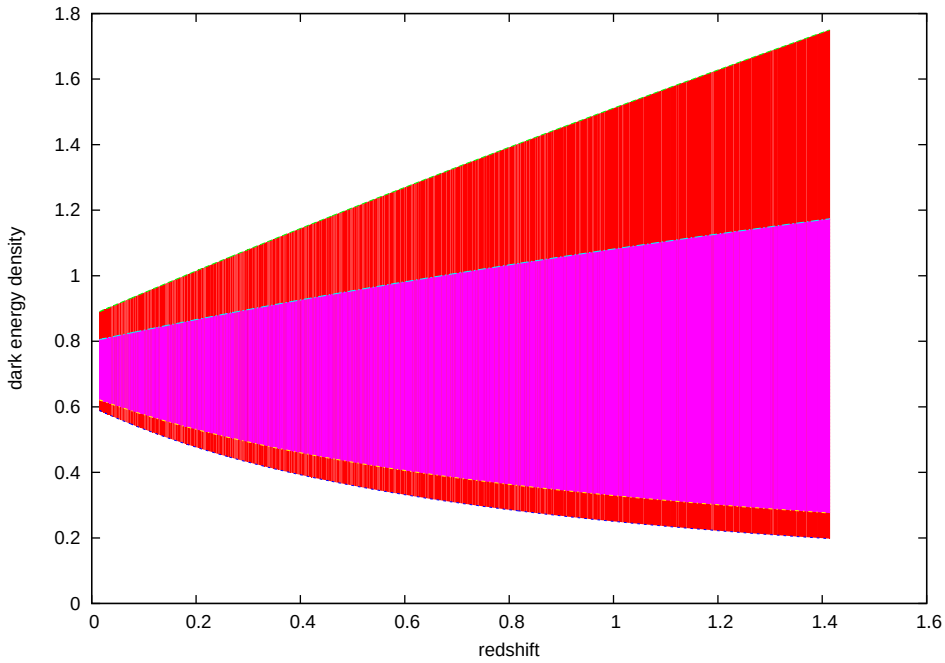

Figure 4.12: $\rho(z)$ v/s z for 1σ and 2σ allowed intervals. The pink region corresponds to 1σ confidence interval and red one represents 2σ confidence intervals

parameters in the equation(Ω_n and w for this equation), the values of these parameters corresponding to 1σ and 2σ confidence intervals of χ^2 of the equation for the previous calculation (eq.(2.7)) is used. For every value of redshift,the value of these (Ω_n and w are used to calculated.
Now, we have the dark energy density calculated for every redshift and the combination of (Ω_n and w for 1σ and 2σ confidence intervals. Now for each confidence interval,maximum and minimum value of ρ_{DE} is calculated and plotted on the same graph. Fig.5.13 represents the dark energy variation with redshift.

4.5.1 Quintessence Model and Observational Constraints

Firstly, we take different values of n and fit it with the data for the potentials. Fig.5.14 represents the contour in $\Omega_{nr} - w$ plane for four values of n i.e. -2, -1, 1 and 2 obtained by analysing supernovae data. Fig.5.15 represent the constraints obtained for BAO data set. Fig.5.16 shows the constraints given

by H(z) data. Fig.5.17 represents the combined constraints obtained from all the three data sets. The combined constraints are obtained by

$$\chi^2_{comb} = \chi^2_{BAO} + \chi^2_{H(z)} + \chi^2_{SnIa} \tag{4.32}$$

All the constraints till now is obtained for inverse potential. Now we obtained the constraints for exponential potential.
Fig.5.18 represents the contour in $\Omega_{nr} - w$ plane for four values of n i.e. -2, -1, 1 and 2 obtained by analysing supernovae data. Fig.5.19 represent the constraints obtained for BAO data set. Fig.5.20 shows the constraints given by H(z) data. Fig.5.21 represents the combined constraints obtained from all the three data sets.
The initial value of w (w_i) varies from -1.0 to -0.33. The lower limit is due to the property of Quintessence model that the minimum value of w can be -1.0. The upper limit is due to the fact that we are analysing the data for dark energy. The value of matter density varies from 0.1 upto 0.5.
The use of wide range of values of w does not create any problem as these equations are very stable and eventually converges to some particular value. In this case, the value of w converges to -1.0.
Fig.5.22 represents the theoretical curves of various values obtained by solving the coupled differential equations against the redshift (z). For the lower redshift (less than 5.0), the curves for different values of α are same and will differ for higher redshift. This means at lower redshift the behaviour of w with redshift is independent of the value of α. This concludes that the constrain obtained by analysing all data sets will be independent of α because the highest redshift of the given data is 2.3.

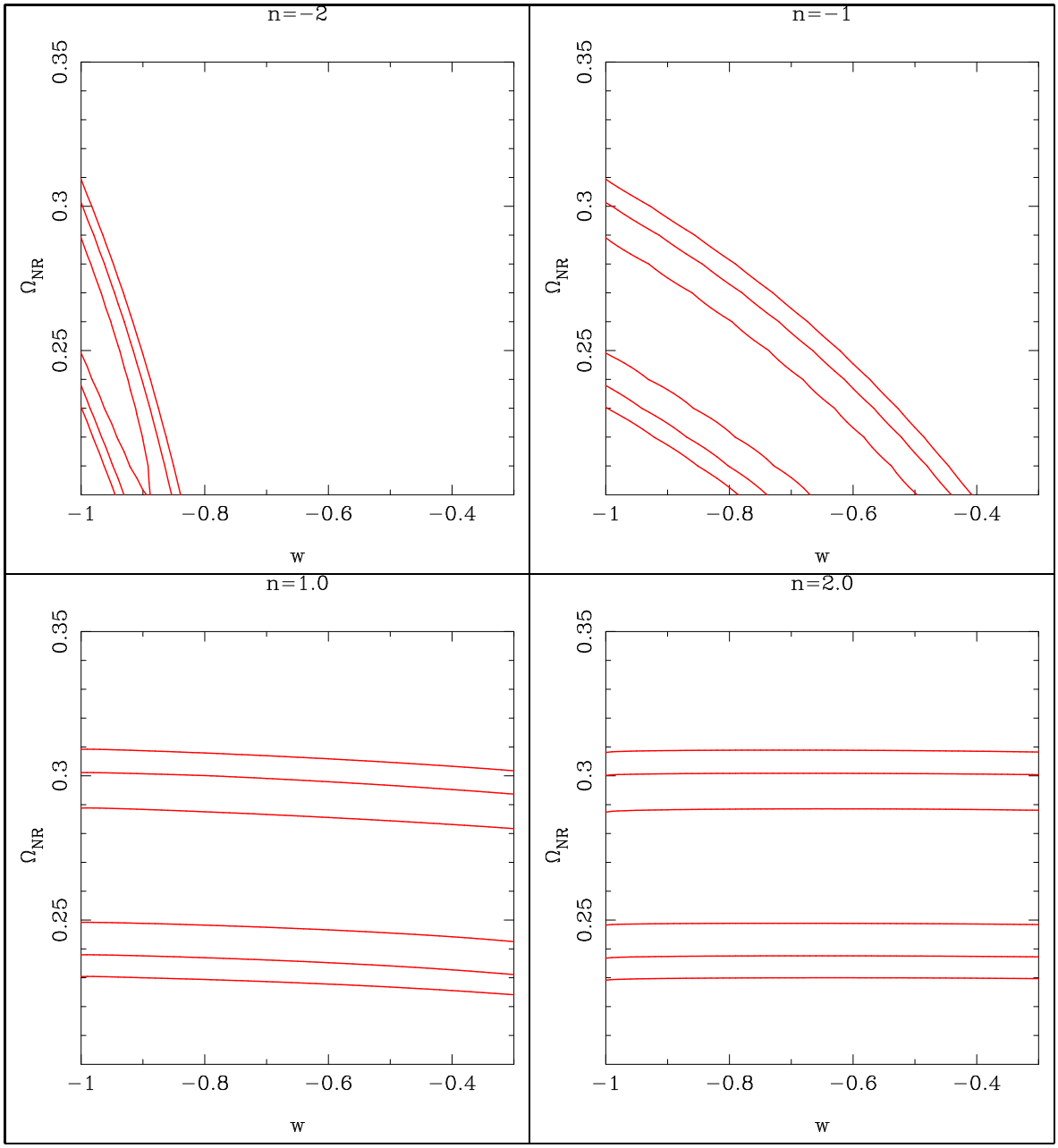

Figure 4.13: Constraints in Ω_{nr}-w plane obtained by supernovae data for different values of n

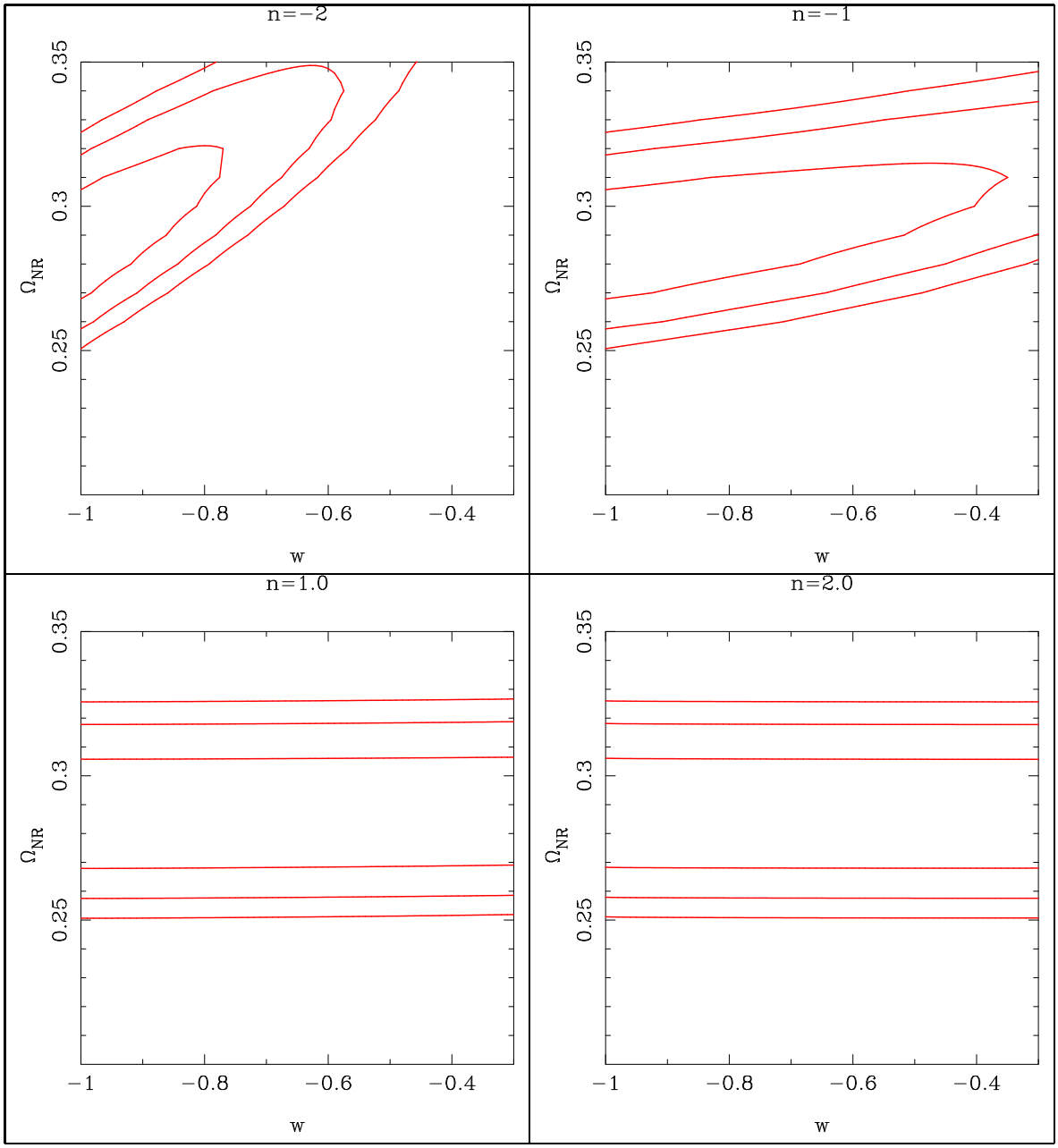

Figure 4.14: Constraints in Ω_{nr}-w plane obtained by BAO data for different values of n

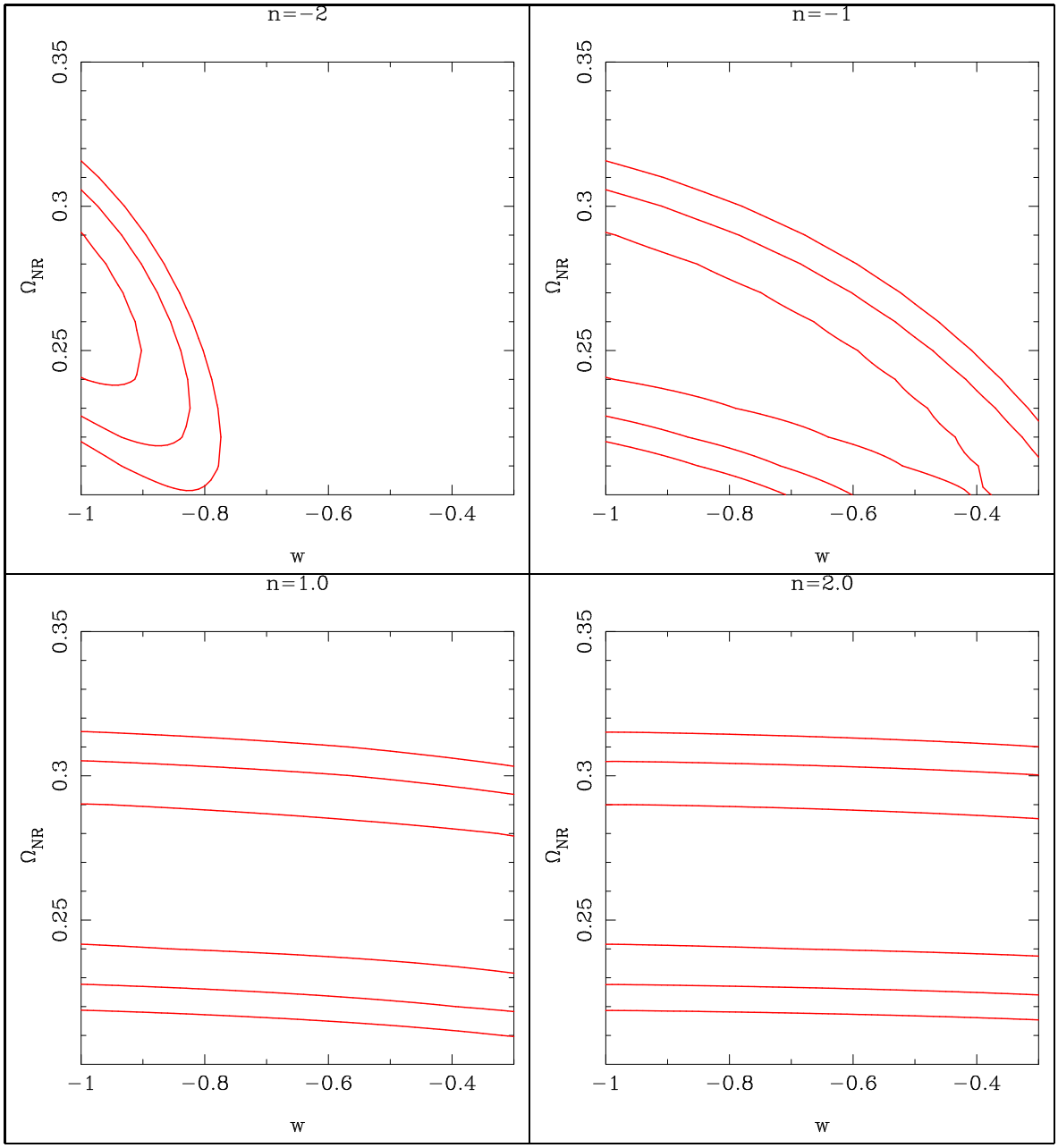

Figure 4.15: Constraints in Ω_{nr}-w plane obtained by Hubble data for different values of n

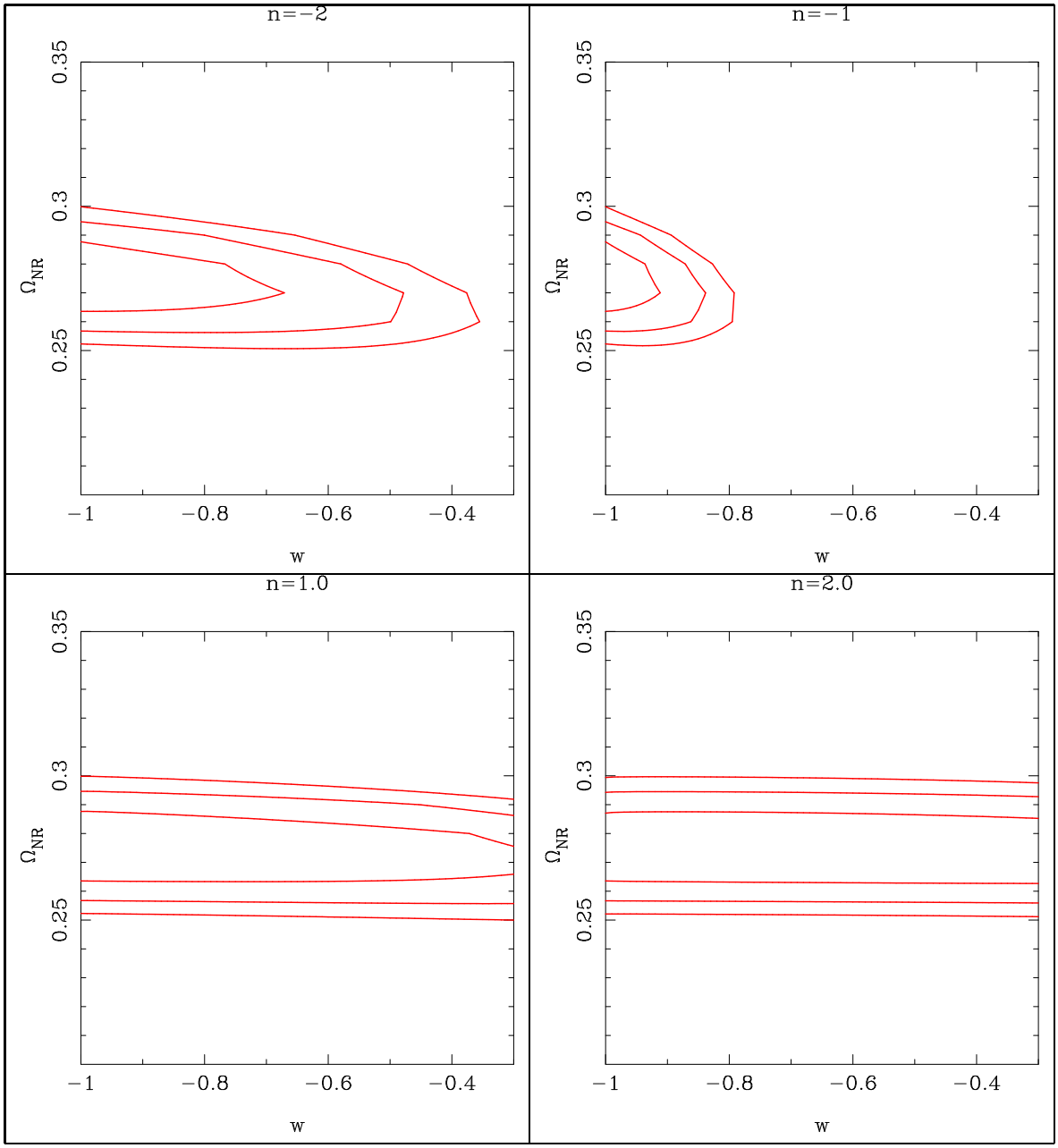

Figure 4.16: Combined Constraints in Ω_{nr}-w plane obtained for different values of n

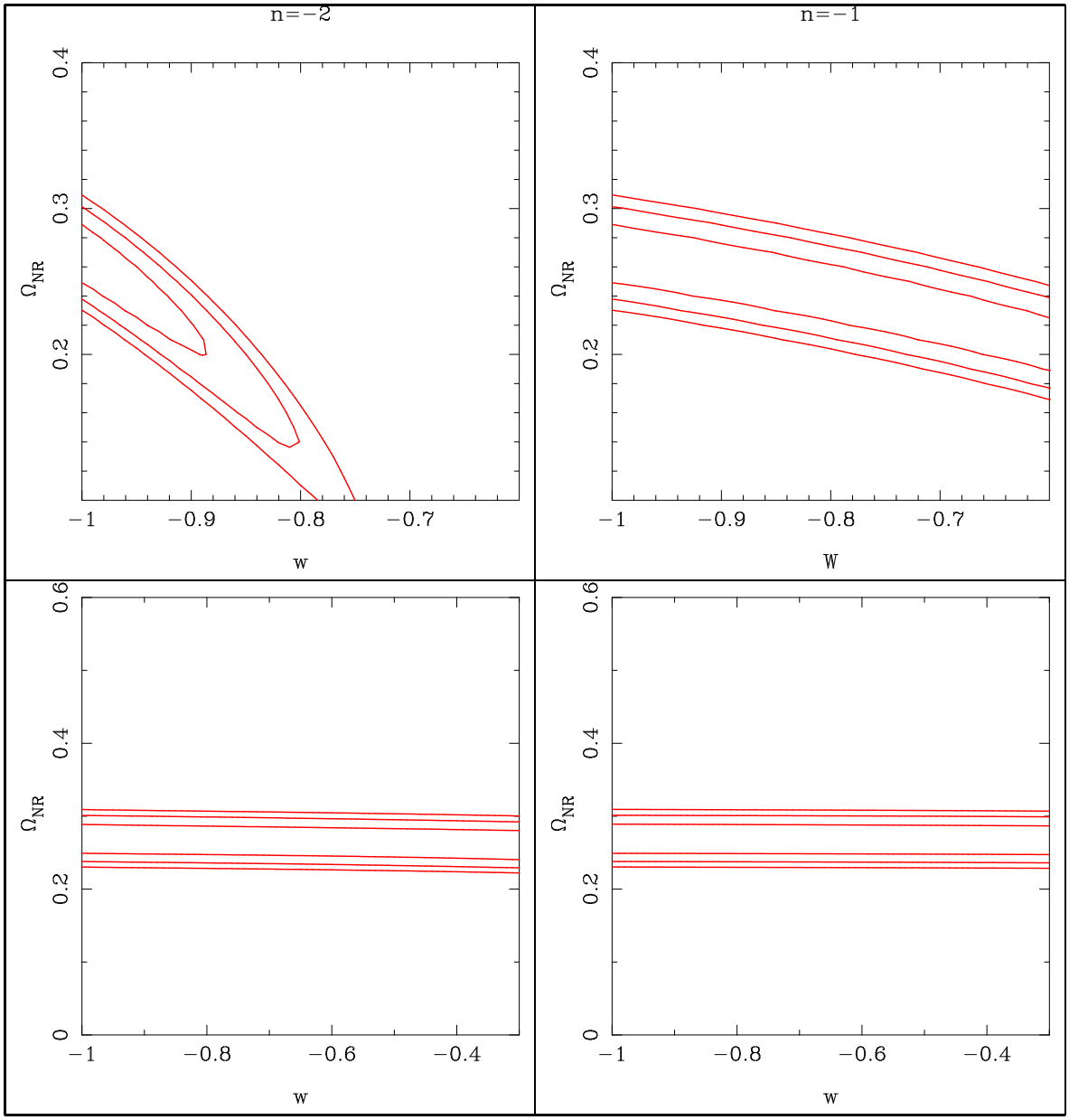

Figure 4.17: Constraints in Ω_{nr}-w plane obtained by supernovae data for exponential potential

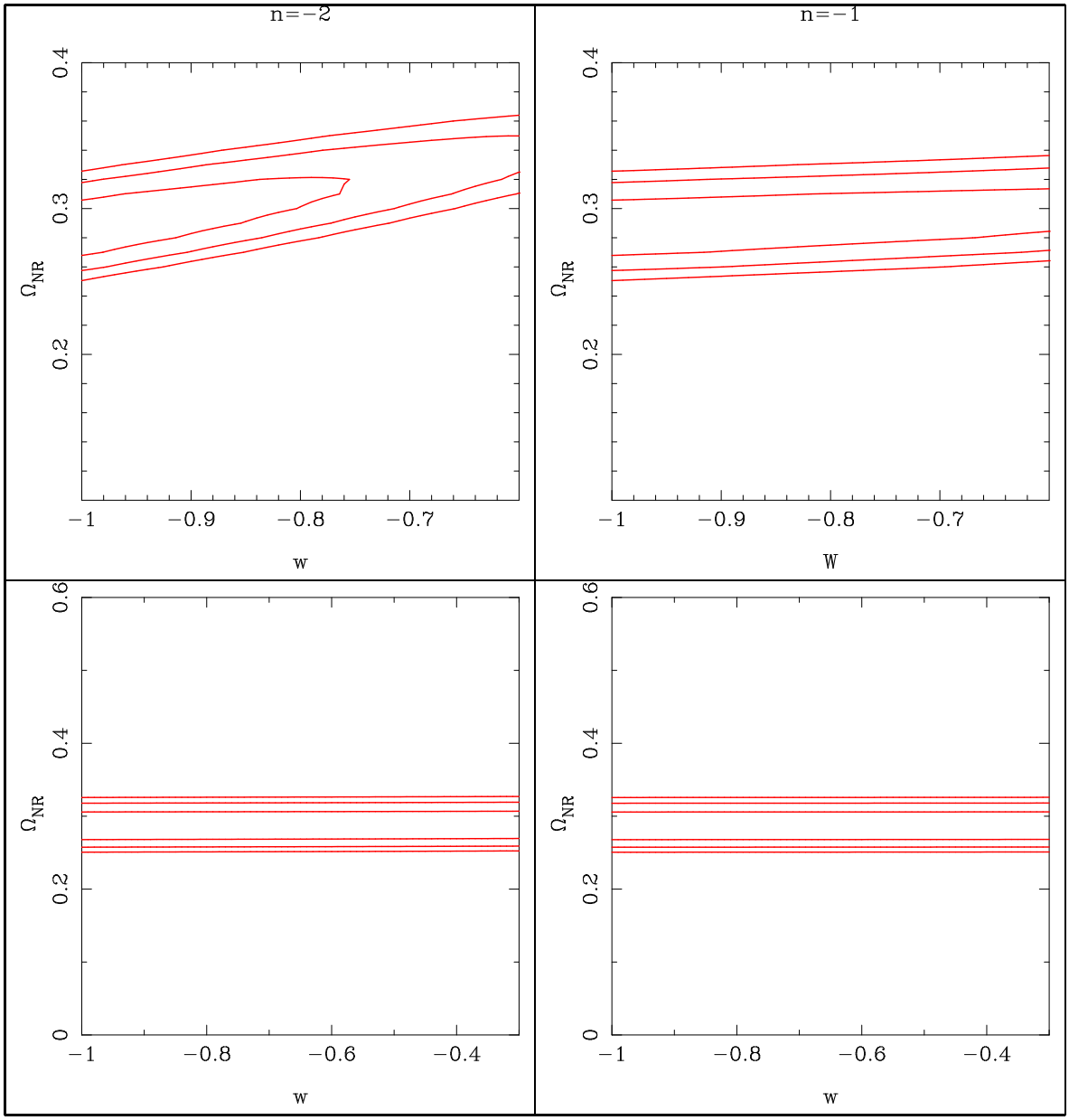

Figure 4.18: Constraints in Ω_{nr}-w plane obtained by BAO data for exponential potential

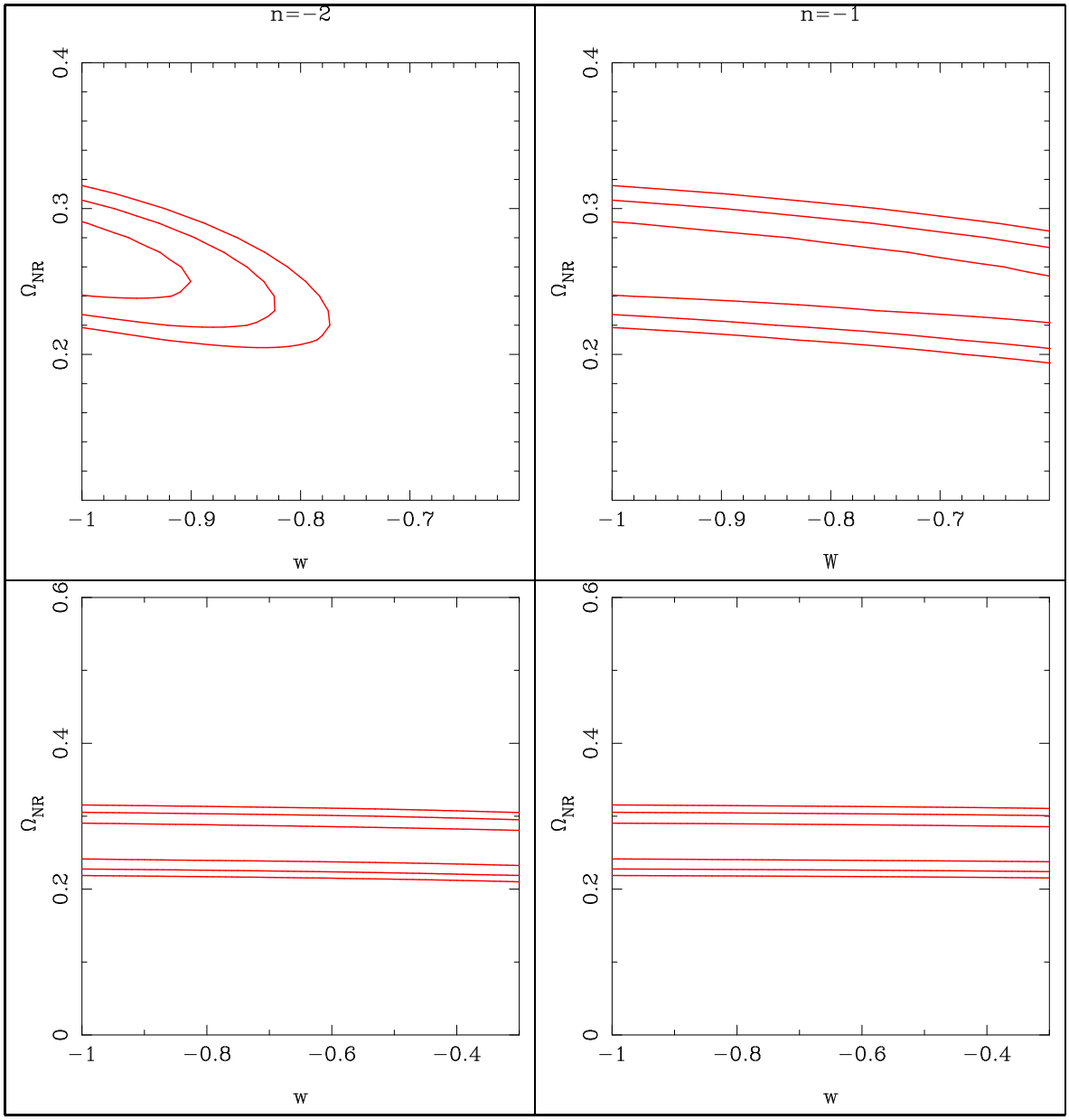

Figure 4.19: Constraints in Ω_{nr}-w plane obtained by Hubble data for exponential potential

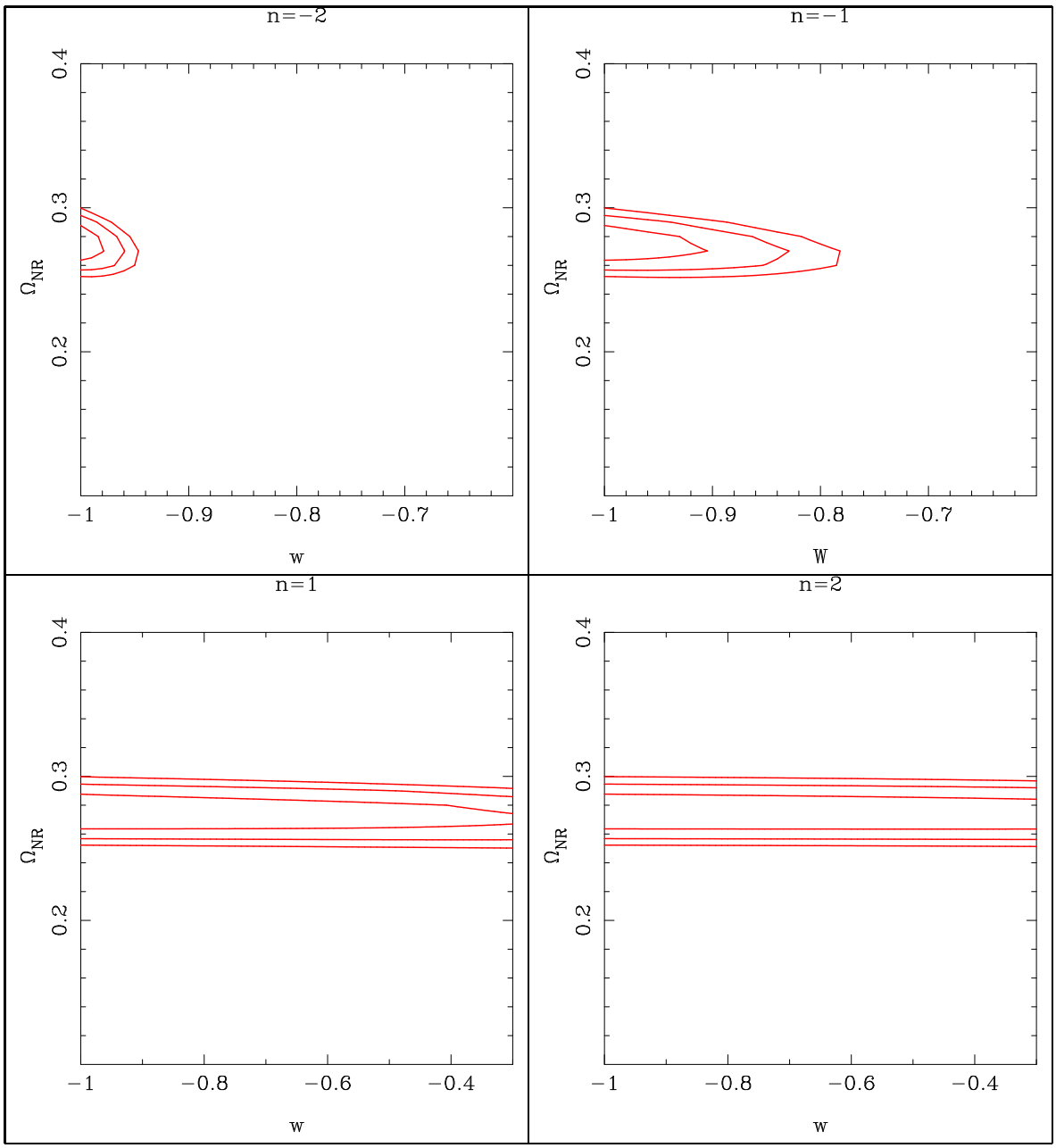

Figure 4.20: Combined Constraints in Ω_{nr}-w plane obtained for different values of n for exponential potential

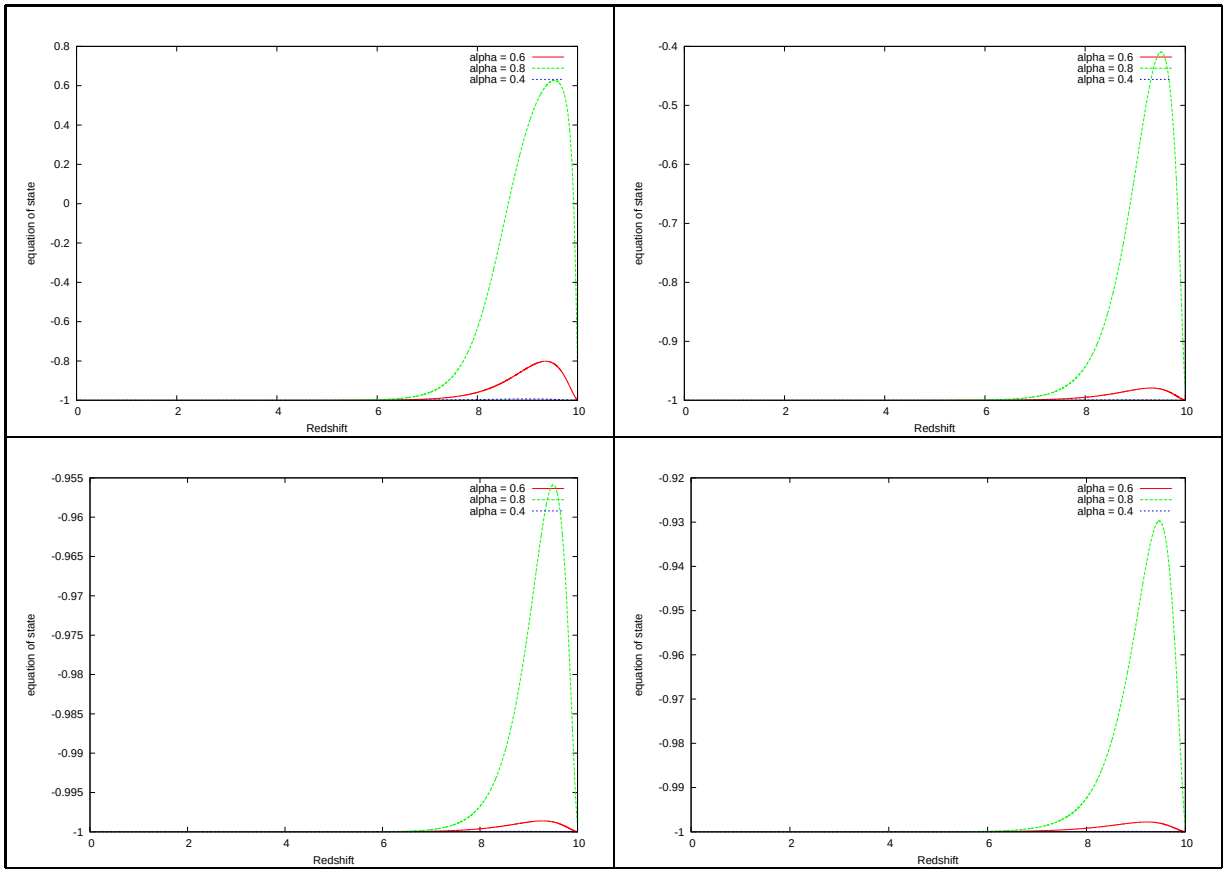

Figure 4.21: Theoretical variation of w with redshift for exponential potential for different values of α(0.4, 0.6, 0.8)

4.6 Combined Constraints

In this section, we compare the constraints obtained by analysing the data sets. We also try to constraint jointly by different data and try to find out whether jointly they put tighter constraints. To constrain the cosmological parameters from the combined constrains of n data sets, we compute

$$\chi^2_{comb} = \Sigma^n_i \chi^2_i \tag{4.33}$$

Where i = 1, 2, 3 is the different data sets taken into consideration. In this case, we have n = 3 and we can compute the χ^2 for all the possible combination of data sets.
Fig.4.22 represents the joint constraint of Supernovae and BAO data (first row) and joint constraints of Supernovae and H(z) data (second row) for spatially flat model. Fig.4.23 represents the joint constraints of BAO and H(z) data (first row) and joint constraints of all the three data sets (second row). By looking at the plot, we can conclude that when we jointly determine the χ^2, the constraints obtained will be tighter. As the supernovae and BAO or H(z) and BAO constraints are complementary to each other, they significantly tighten the constraints.
Fig.4.24 represents the comparison between the joint constraints obtained by different combinations of data sets taken two at a time with the joint constraints obtained by analysing all data sets jointly. If we consider the distance between the points (the coordinates of minimum χ^2) in the plot as a measurement of consistency, the lower left plot which compare the joint constraint of all the three data sets with joint constraint of Supernovae and BAO data has the two point closest to each other. We can conclude that joint constraint of Supernovae and BAO is the most consistent combination with the combination of all of them. In other words, adding of constraints by H(z) data does not have any profound effect on tightening the constraints.
Fig.4.25 represents the joint constraint of Supernovae and BAO data (first row) and joint constraints of BAO and H(z) data (second row) for non-flat universe. Fig.4.26 represents the joint constraints of Supernovae and H(z) data (first row) and joint constraints of all the three data sets (second row). We can infer that the effect of tightening of constraints is not as effective as in the case of spatially flat model and the tightening is worst in the last case (SNIa + H(z)).
Fig.4.27 represents the comparison between the joint constraints obtained

by different combinations of data sets taken two at a time with the joint constraints obtained by analysing all data sets jointly. Here the distance between the points of minimum χ^2 do not change significantly but in the case of comparison of SNIa+BAO constraints with the joint constraints, the contours are almost overlapping.

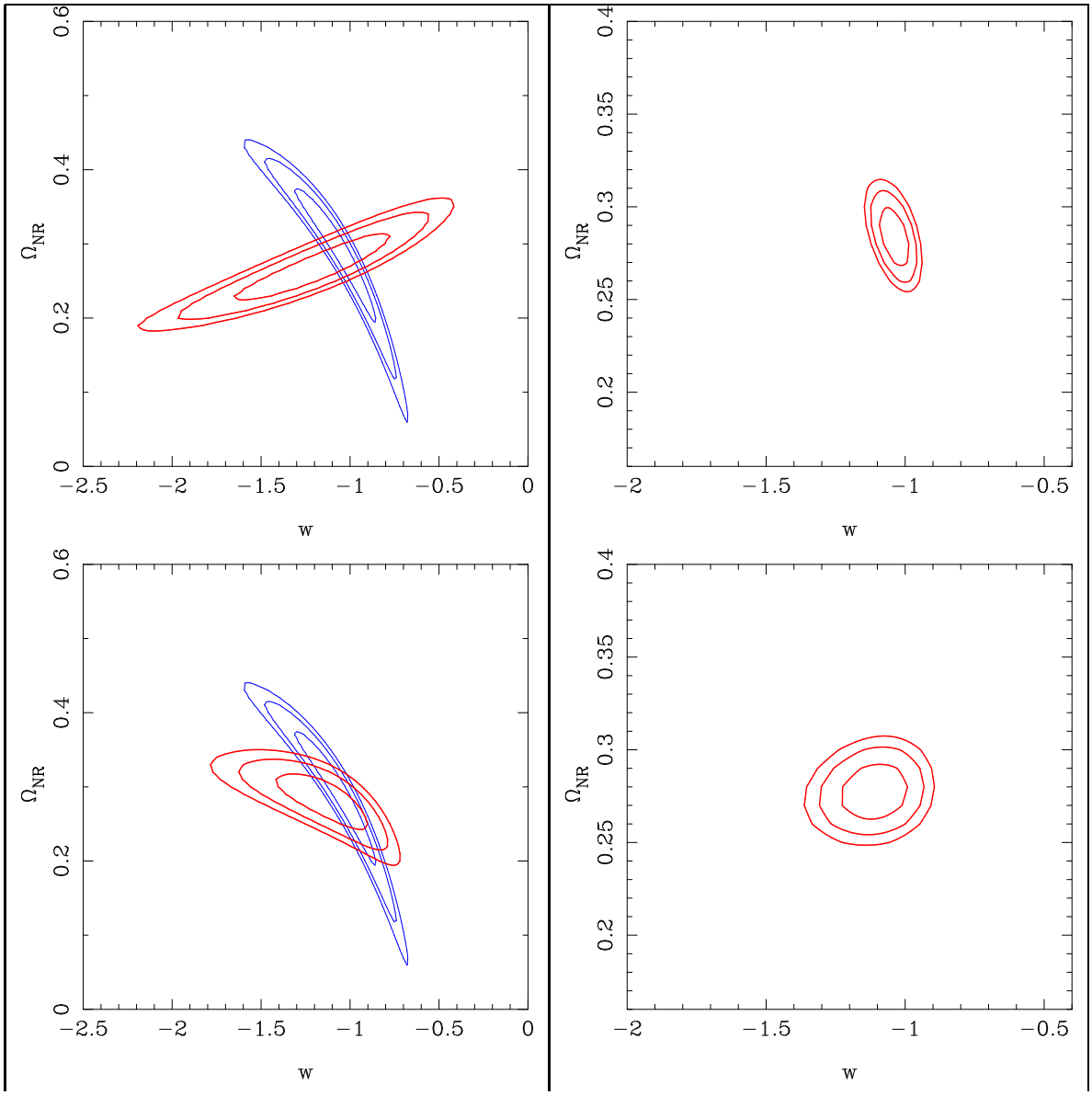

Figure 4.22: The upper left plot represents the constraints obtained by Supernovae and BAO data on the same graph and the plot right to it represents joint constraints of Supernovae and BAO data. The lower left plot represents the constraints obtained by H(z) and BAO data on the same graph and the plot right to it represents joint constraints of H(z) and BAO data

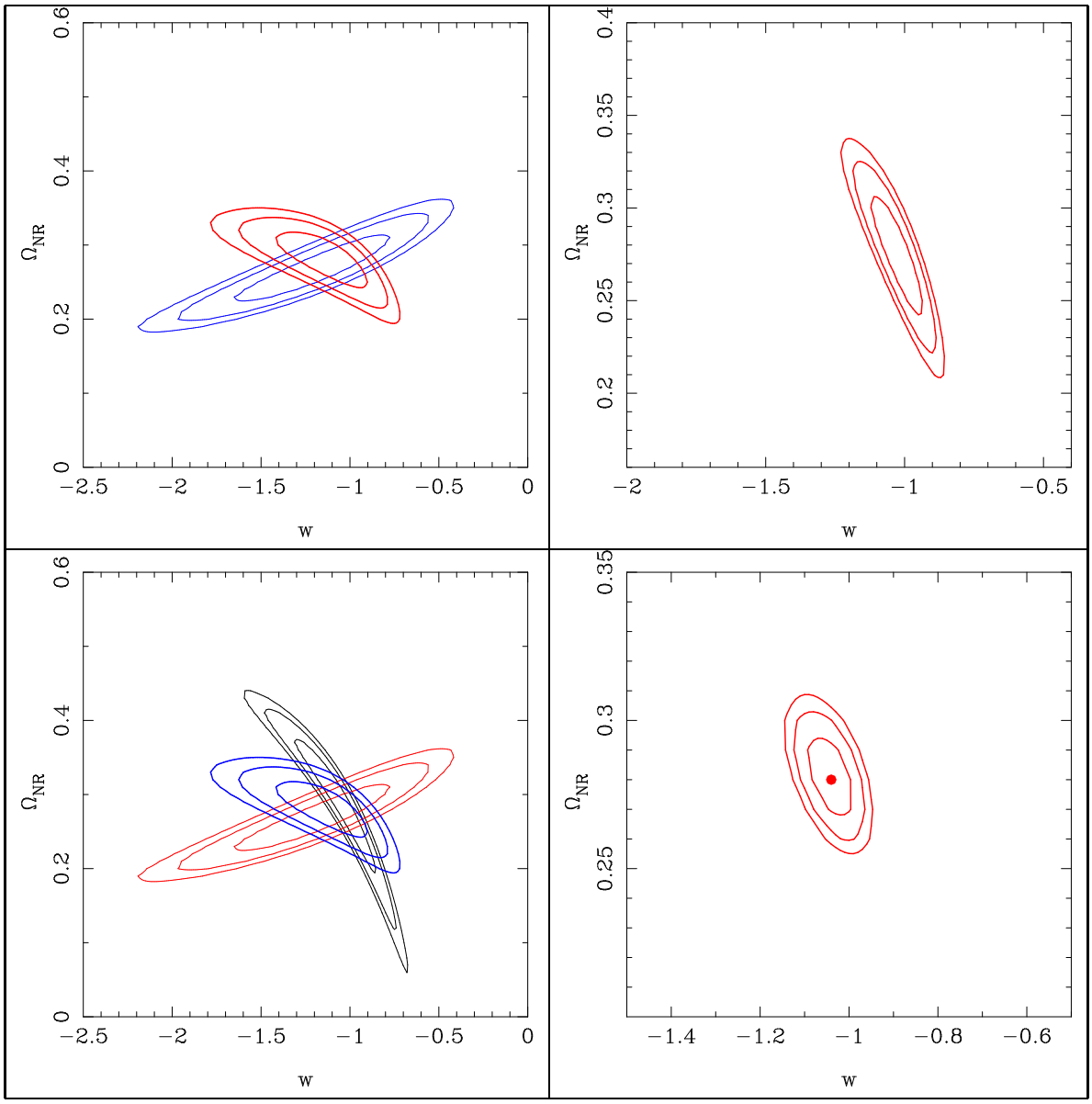

Figure 4.23: The upper left plot represents the constraints obtained by Supernovae and H(z) data on the same graph and the plot right to it represents joint constraints of Supernovae and H(z) data. The lower left plot represents the constraints obtained by Supernovae, H(z) and BAO data on the same graph and the plot right to it represents joint constraints of all the three data sets.

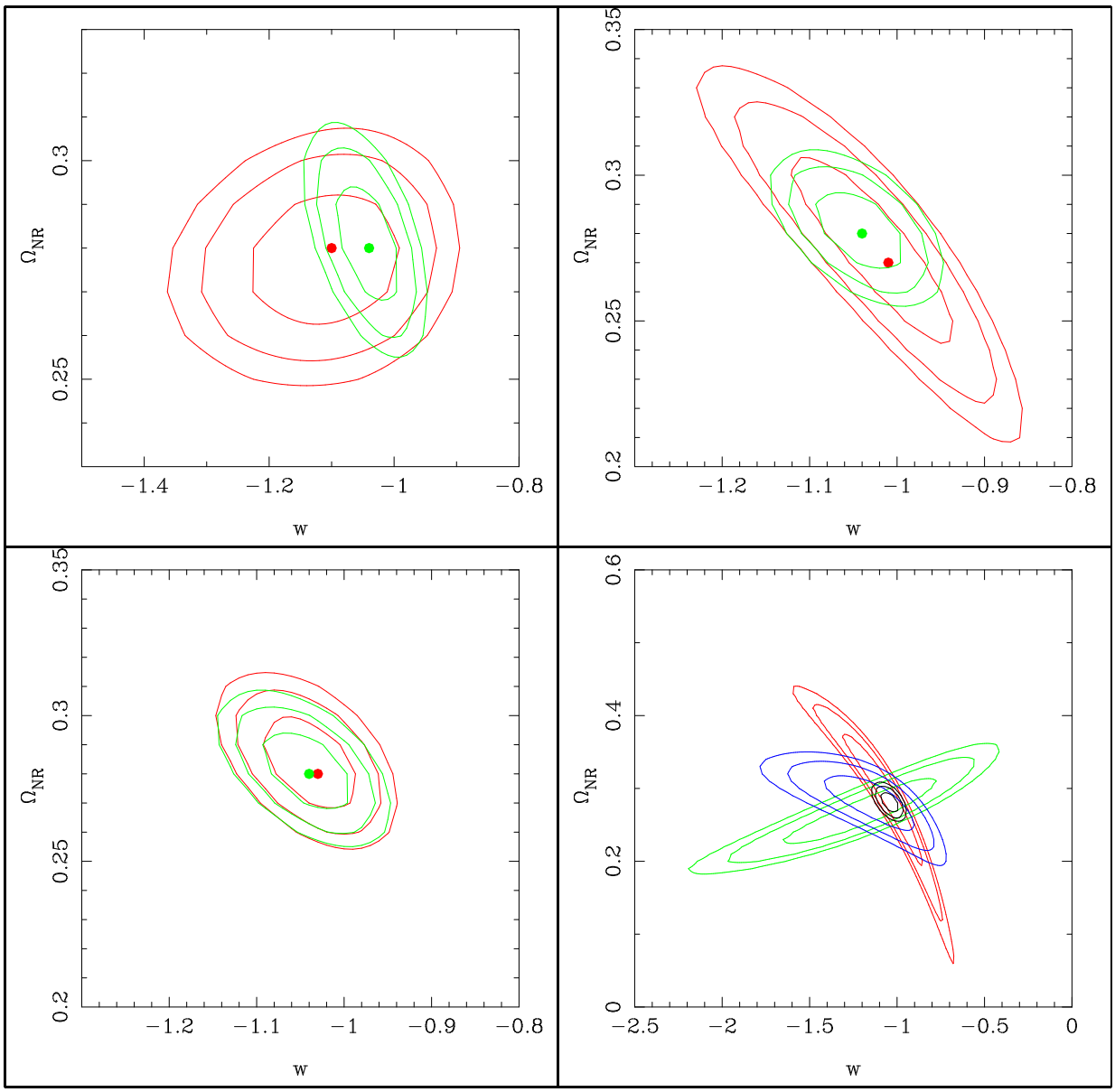

Figure 4.24: The upper left plot represents the comparison of joint constraints of three data sets with the joint constraints with BAO and H(z) data. The upper right plot represents the comparison of joint constraints of three data sets with the joint constraint of Supernovae and H(z) data and the lower left with the joint constraints of Supernovae and BAO data. The lower right represents the joint constraint with the constraints from all the three data sets.

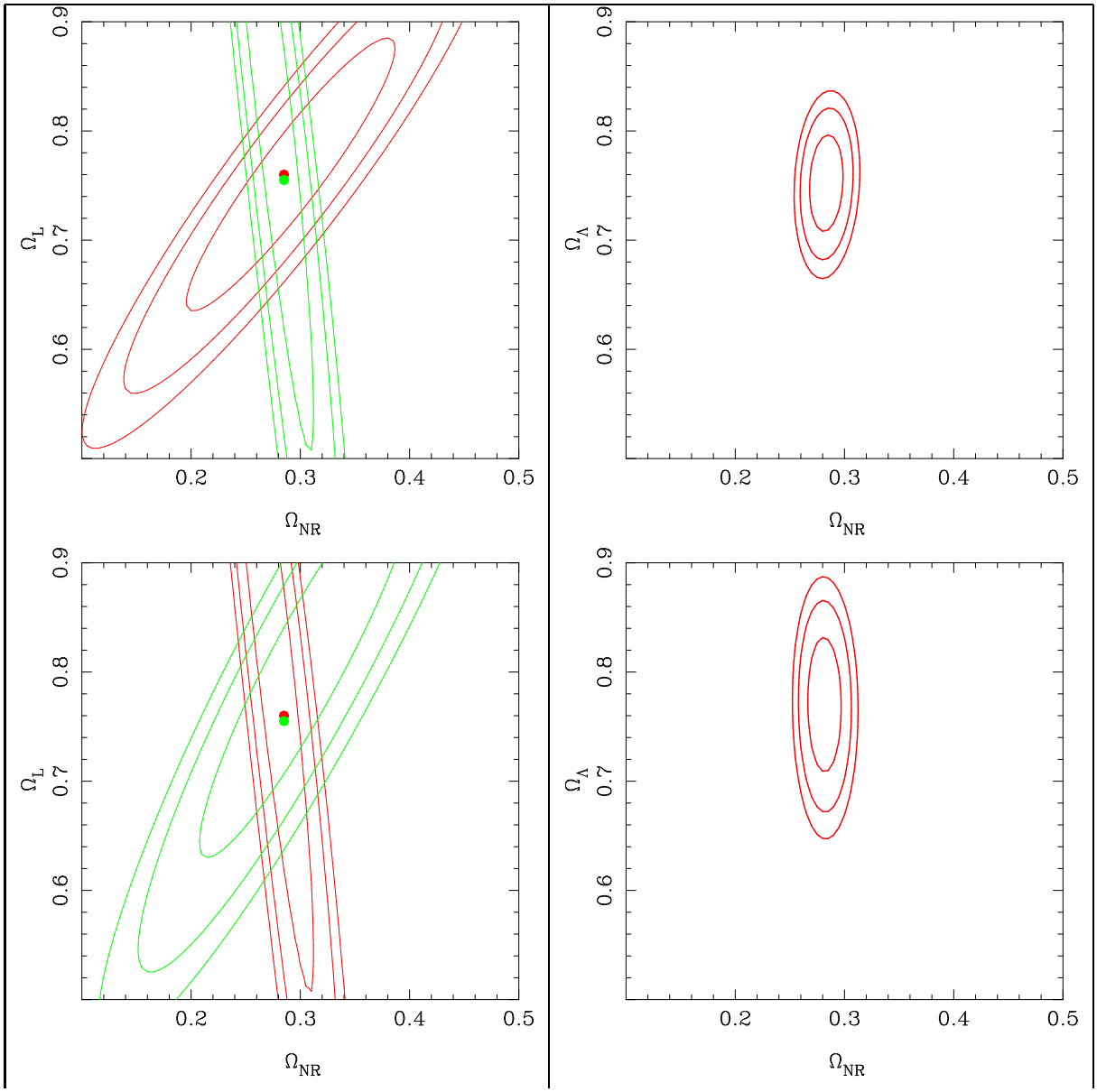

Figure 4.25: Constraints for non-flat universe.The upper left plot represents the constraints obtained by Supernovae and BAO data on the same graph and the plot right to it represents joint constraints of Supernovae and BAO data. The lower left plot represents the constraints obtained by H(z) and BAO data on the same graph and the plot right to it represents joint constraints of H(z) and BAO data

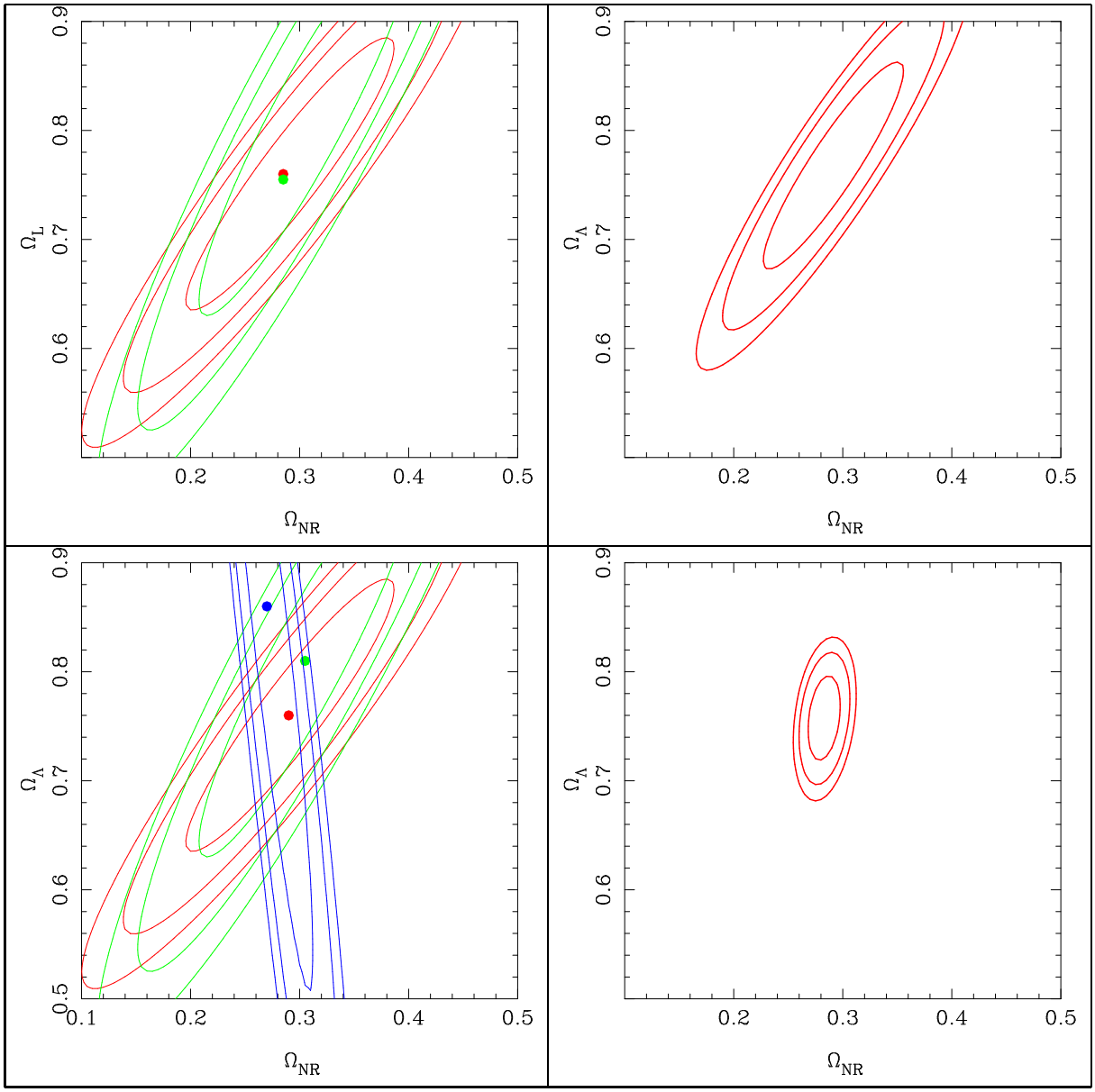

Figure 4.26: Constraints for non-flat universe. The upper left plot represents the constraints obtained by Supernovae and H(z) data on the same graph and the plot right to it represents joint constraints of Supernovae and H(z) data. The lower left plot represents the constraints obtained by Supernovae, H(z) and BAO data on the same graph and the plot right to it represents joint constraints of all the three data sets.

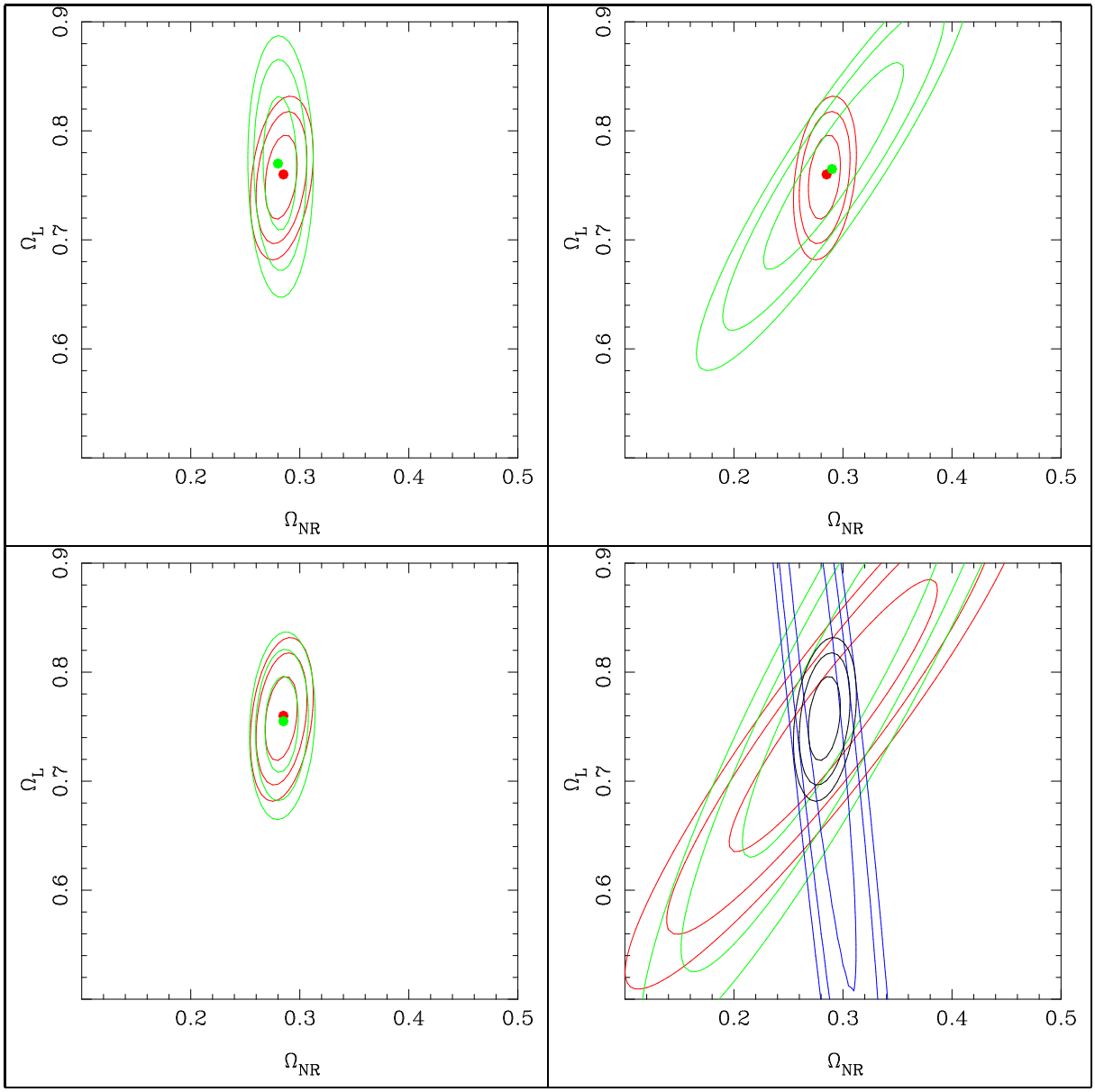

Figure 4.27: Constraints for non-flat universe. The upper left plot represents the comparison of joint constraints of three data sets with the joint constraints with BAO and H(z) data. The upper right plot represents the comparison of joint constraints of three data sets with the joint constraint of Supernovae and H(z) data and the lower left with the joint constraints of Supernovae and BAO data. The lower right represents the joint constraint with the constraints from all the three data sets.

Chapter 5

Conclusions

In this thesis, we used three different probes i.e. Supernovae data, BAO data and H(z) data to constrain a number of spatially flat and non-flat models. From different combinations of data sets, different constraints have been obtained for the different models we consider. We can conclude that the joint analysis of data gives tighter constraints compared to the individual analysis of data sets. We can also infer that more data and more precise data is required to tightly pin down the spatial curvature of the Universe in dynamical dark energy models.

One of the key features is that we used the particle physics scalar field models to determine the equation of state w and then constrain its value with the observations. This is important because we can use the established models of particle physics to constrain the parameters in cosmology.

One can put observational constraints on various cosmology models. We consider only cannonical scalar field model. Using same technique, we can put constrains on various scalar field models. Thus, observations play significant role in determining the viable cosmology.

We also consider the dark energy models with space curvature with constant equation of state. It would be of significant interest to determine the constraints on space curvature in the non-flat model from CMB anisotropy measurements. Such an analysis, possibly in combination with that of other data of the kind considered here could go a long way towards establishing

whether space curvature contributes significantly to the current cosmological energy budget.

The analysis can be extended to other cosmologies with scalar field models like k-essence, tachyon etc. We will analyse other potential forms in scalar field models determine the constraints on space curvature in the non-flat model from CMB anisotropy measurements.

Bibliography

[1] Muhammad Omer Farooq. Observational Constraints On Dark Energy Cosmological Model Parameters; final thesis, Kansas State University, 2013.

[2] Maddumage Don P. Hemantha, Yun Wang.Measurement of H(z) and DA (z) from the two-dimensional power spectrum of Sloan Digital Sky Survey luminous red galaxies; http://arxiv.org/abs/1310.6468v1

[3] H.K.Jassal, J.S.Bagla and T.Padmanabhan; Observational constraints on low redshift evolution of dark energy: How consistent are different observations? http://arXiv.org/abs/astro-ph/0506748v2

[4] T.Padmanabhan; Theoretical Astrophysics Volume 3: Galaxies and Cosmology.

[5] Y. Chen and B. Ratra. Hubble parameter data constraints on dark energy; Physics Letters B, 703:406–411, September 2011.

[6] Omer Farooq and Bharat Ratra. Constraints on dark energy from the lyα forest baryon acoustic oscillations measurement of the redshift 2.3 hubble parameter; Physics Letters B, 723(13):1 – 6, 2013.

[7] E. Gaztaaga, A. Cabr, and L. Hui; Clustering of luminous red galaxies-IV. Baryon acoustic peak in the line-of-sight direction and a direct measurement of H(z); MNRAS, 399:1663–1680.

[8] James B. Hartle. Gravity: An introduction to Einstein's general relativity; Addison-Wesley, 2003.

[9] S. Weinberg. Gravitation and cosmology: principles and applications of the general theory of relativity. Wiley, 1972.

[10] Steven Weinberg. The cosmological constant problem. Rev. Mod. Phys., 61:1–23, Jan 1989.

[11] A.R. Liddle. An introduction to modern cosmology; Wiley, 2003.

[12] Data Mania. Constraints on the dark energy models from observational data; Master's thesis, Kansas State University, 2012.

[13] Edmund J. Copeland, M.Sami and Shinji Tsujikawa; Dynamics of dark energy;

[14] S. Capozziello, V.F. Cardone, E. Piedipalumbo, C. Rubano; Dark energy exponential potential models as curvature quintessence; http://arxiv.org/abs/astro-ph/0507438v1.

[15] Suzuki et.al. http://arxiv.org/abs/1105.3470

[16] Kowalski et.al. First Union Compilation;

[17] Amanullah et.al. The Union2 compilation;

[18] X. Xu, A. J. Cuesta, N. Padmanabhan, D. J. Eisenstein, and C. K. McBride. Measuring DA and H at z=0.35 from the SDSS DR7 LRGs using baryon acoustic oscillations. MNRAS, 431:2834–2860, May 2013.

[19] Chris Blake, Eyal A. Kazin, Florian Beutler, Tamara M. Davis, David Parkinson, Sarah Brough, Matthew Colless, Carlos Contreras, Warrick Couch, Scott Croom, Darren Croton, Michael J. Drinkwater, Karl Forster, David Gilbank, Mike Gladders, Karl Glazebrook, Ben Jelliffe, Russell J. Jurek, I-hui Li, Barry Madore, D. Christopher Martin, Kevin Pimbblet, Gregory B. Poole, Michael Pracy, Rob Sharp, Emily Wisnioski, David Woods, Ted K. Wyder, and H. K. C. Yee. The wigglez dark energy survey: mapping the distance redshift relation with baryon acoustic oscillations. Monthly Notices of the Royal Astronomical Society, 418(3):1707–1724, 2011.

[20] N. Suzuki, D. Rubin, C. Lidman, G. Aldering, R. Amanullah, K. Barbary, L. F. Bar- rientos, J. Botyanszki, M. Brodwin, N. Connolly, K. S. Dawson, A. Dey, M. Doi, M. Donahue, S. Deustua, P. Eisenhardt, E. Ellingson, L. Faccioli, V. Fadeyev, H. K. Fakhouri, A. S. Fruchter, D. G. Gilbank, M. D. Gladders, G. Goldhaber, A. H. Gon- zalez, A. Goobar,

A. Gude, T. Hattori, H. Hoekstra, E. Hsiao, X. Huang, Y. Ihara, M. J. Jee, D. Johnston, N. Kashikawa, B. Koester, K. Konishi, M. Kowalski, E. V. Linder, L. Lubin, J. Melbourne, J. Meyers, T. Morokuma, F. Munshi, C. Mullis, T. Oda, N. Panagia, S. Perlmutter, M. Postman, T. Pritchard, J. Rhodes, P. Ripoche, P. Rosati, D. J. Schlegel, A. Spadafora, S. A. Stanford, V. Stanishev, D. Stern, M. Stro- vink, N. Takanashi, K. Tokita, M. Wagner, L. Wang, N. Yasuda, H. K. C. Yee, and T. Supernova Cosmology Project. The Hubble Space Telescope Cluster Supernova Survey. V. Improving the Dark-energy Constraints above z $>$ 1 and Building an Early-type-hosted Supernova Sample. ApJ, 746:85, February 2012.